

FCIC pyrolysis modeling

Gavin Wiggins
wigginsg@ornl.gov

September 20, 2021

Contents

| | | |
|----------|---|-----------|
| 1 | Introduction | 2 |
| 2 | Experimental apparatus and data | 2 |
| 2.1 | Apparatus | 2 |
| 2.2 | Feedstock proximate and ultimate analyses | 5 |
| 2.3 | Feedstock chemical analysis | 7 |
| 2.4 | Bed particle characteristics | 10 |
| 2.5 | Product yields | 11 |
| 3 | Model development | 13 |
| 3.1 | Basis of analysis | 13 |
| 3.2 | Biomass pyrolysis kinetics | 14 |
| 3.3 | Biomass composition | 17 |
| 3.4 | Batch reactor and CSTR models | 19 |
| 4 | Results and discussion | 21 |
| 4.1 | Feedstock characterization | 21 |
| 4.2 | Batch reactor model | 33 |
| 4.3 | CSTR model | 39 |
| 5 | Conclusions | 39 |
| 6 | Hardware requirements | 39 |
| 7 | Source code and web application | 40 |

1 Introduction

This report discusses biomass pyrolysis fluidized bed reactor modeling activities for the Feedstock-Conversion Interface Consortium (FCIC) project. Model parameters are based on the NREL 2FBR biomass fast pyrolysis system which is comprised of a two-inch diameter bubbling fluidized bed (BFB) reactor. Experiment data, apparatus information, and material data are provided by the National Renewable Energy Laboratory (NREL), the National Energy Technology Laboratory (NETL), and the Idaho National Laboratory (INL). Model development and associated results are provided by Oak Ridge National Laboratory (ORNL).

2 Experimental apparatus and data

Information about the fluidized bed reactor such as typical operating conditions and reactor geometry is provided in this section. Data pertaining to proximate and ultimate analysis, chemical analysis, and particle characteristics for each feedstock are also presented. Characteristics of the bed particles are also provided. Lastly, measured product yields from the fast pyrolysis of each feedstock are given in this section too.

2.1 Apparatus

The BFB pyrolysis reactor at NREL is operated at fast pyrolysis conditions to thermochemically convert biomass feedstock into gas, tar, and char products. Pyrolysis occurs in a fluidized bed reactor comprised of a bed of sand fluidized by nitrogen gas. Biomass particles are fed into the bed via an auger and secondary gas stream at the side of the reactor. An overview of the components and flows related to the pyrolysis reactor (pyrolyzer) is given in Figure 1. The diagram was created using information provided by NREL [4].



Figure 1: Components (left) and inlet/outlet flows (right) of the NREL bubbling fluidized bed pyrolysis reactor.

Dimensions for the reactor tube, feed inlet, insulation, heat jacket, and distributor plate are given in Figure 2 and Table 1. The main reactor tube is a 2-inch Schedule 40 pipe; therefore, the inner and outer reactor diameters are determined from nominal pipe size tables. The gas distributor contains 18 holes in a triangular pattern [4].

Typical operating conditions of the pyrolyzer are presented in Table 2. Pressure drop across the distributor is about 80-90 inches of H_2O . Nitrogen gas is used to fluidize the bed and assist biomass particles through the feed inlet tube. Experiments are conducted with an initial mass of sand in the bed; sand is not fed into the reactor during operation. Insulation surrounds the reactor while heat jackets extend almost the entire height of the unit. A cooling jacket surrounds the feed inlet tube. Pyrolysis vapors exit directly out the top of the reactor via a straight tube [4].

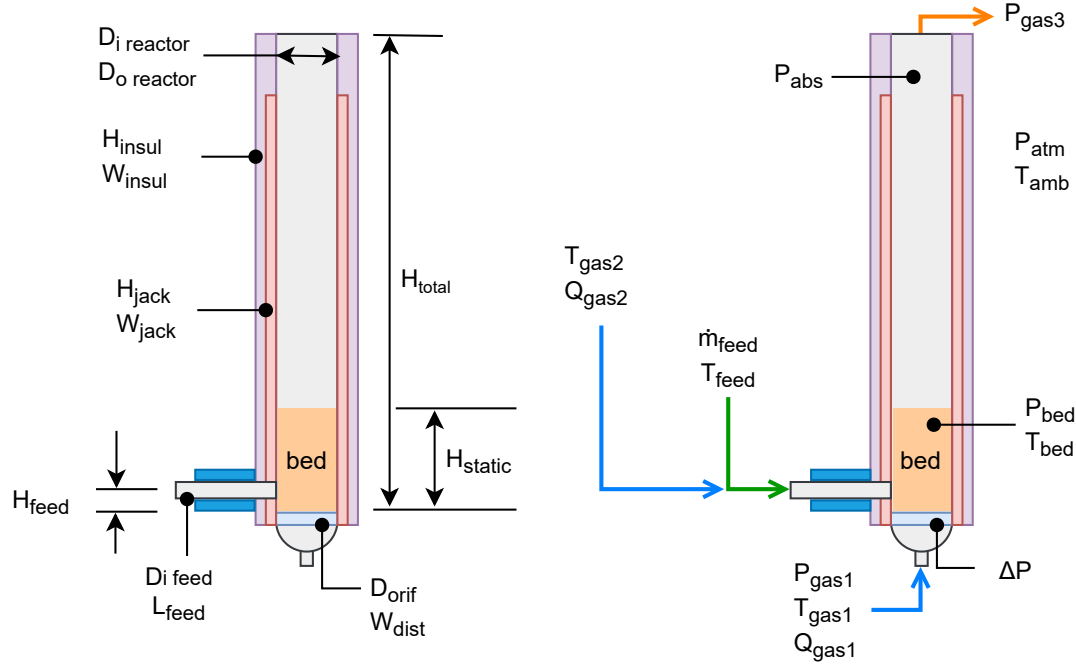


Figure 2: Dimensions and typical fast pyrolysis operating conditions for the NREL 2FBR pyrolyzer reactor.

Table 1: Dimensions for components of the fluidized bed pyrolysis reactor.

| Reactor dimension | Symbol | Value | Units |
|-------------------------------------|--------------------------|-------|-------|
| Inner reactor diameter | $D_{i, \text{ reactor}}$ | 5.25 | cm |
| Outer reactor diameter | $D_{o, \text{ reactor}}$ | 6.03 | cm |
| Static bed height | H_{static} | 10.16 | cm |
| Total reactor height | H_{total} | 43.18 | cm |
| Feed inlet inner diameter | $D_{i, \text{ feed}}$ | 1.27 | cm |
| Feed height from top of distributor | H_{feed} | 1.9 | cm |
| Feed inlet tube length | L_{feed} | 18.29 | cm |
| Insulation height | H_{insul} | 43.18 | cm |
| Insulation thickness | W_{insul} | 10 | cm |
| Jacket height | H_{jack} | 35 | cm |
| Jacket thickness | W_{jack} | 5 | cm |
| Diameter of distributor orifices | D_{orif} | 0.08 | cm |
| Thickness of distributor plate | W_{dist} | 3.17 | mm |
| Number of orifices in distributor | n | 18 | – |

Table 2: Typical operating conditions for the fluidized bed pyrolysis reactor. Atmospheric pressure considers elevation of NREL site in Golden, CO.

| Reactor condition | Symbol | Value | Units |
|--------------------------------|-------------------------|---------|-----------------|
| Absolute pressure in reactor | P_{abs} | 101.3 | kPa |
| Atmospheric pressure | P_{atm} | 81 | kPa |
| Ambient air temperature | T_{amb} | 300.15 | K |
| Absolute bed pressure | P_{bed} | 115 | kPa |
| Bed temperature | T_{bed} | 773.15 | K |
| Pressure drop over distributor | ΔP | 21.17 | KPa |
| Absolute inlet gas pressure | P_{gas1} | 110–140 | kPa |
| Inlet gas temperature | T_{gas1} | 773.15 | K |
| Inlet gas flowrate | Q_{gas1} | 14 | SLM (0.29 g/s) |
| Secondary gas temperature | T_{gas2} | 298.15 | K |
| Secondary gas flowrate | Q_{gas2} | 1.4 | SLM (0.029 g/s) |
| Absolute outlet gas pressure | P_{gas3} | 90–110 | kPa |
| Biomass inlet feedrate | \dot{m}_{feed} | 420 | g/hr |
| Biomass inlet temperature | T_{feed} | 298.15 | K |

2.2 Feedstock proximate and ultimate analyses

Proximate and ultimate analysis measurements for each feedstock are given in Tables 3 and 4 on an as-determined basis (ad). A visual comparison of the proximate and ultimate analysis measurements is shown in Figure 3. Overall, the elemental composition of each feedstock is similar based on the ultimate analysis data. Differences in elemental fractions occur mainly in the C and O fractions with a maximum difference of approximately 3 wt.% and 5 wt.% respectively. For the proximate analysis fractions, the largest differences are observed for the fixed carbon (FC) and volatile matter (VM) at 10 wt.% and 13 wt.% respectively. A maximum difference of about 3 wt.% is seen for the ash and moisture fractions.

Table 3: Proximate analysis measurements given as wt. % as-determined basis.

| Name | Cycle | FC | VM | Ash | Moisture | Total |
|-----------------------------|-------|-------|-------|------|----------|--------|
| Residues | 1 | 20.72 | 72.92 | 1.45 | 4.92 | 100.01 |
| Stem wood | 2 | 16.79 | 79.40 | 0.28 | 3.55 | 100.02 |
| Bark | 3 | 27.16 | 66.29 | 0.70 | 5.86 | 100.01 |
| Needles | 4 | 23.26 | 69.54 | 3.78 | 3.42 | 100.00 |
| Bark + needles | 5 | 24.35 | 68.30 | 2.52 | 4.85 | 100.02 |
| Residues (rep 1) | 8 | 20.78 | 72.37 | 1.65 | 5.20 | 100.00 |
| Residues:bark:needles 1:1:1 | 10 | 23.75 | 69.02 | 2.05 | 5.19 | 100.01 |
| Residues:bark:needles 1:2:2 | 11 | 24.12 | 68.57 | 2.02 | 5.29 | 100.00 |
| Air classified (10 Hz) | 12 | 19.92 | 75.59 | 0.92 | 3.57 | 100.00 |
| Air classified (28 Hz) | 13 | 18.68 | 76.31 | 0.61 | 4.41 | 100.01 |
| Whole tree (13 yr) | 15 | 19.15 | 76.72 | 0.44 | 3.71 | 100.02 |
| Stem wood (13 yr) | 16 | 18.60 | 78.37 | 0.30 | 2.75 | 100.02 |
| Maximum difference | | 10.37 | 13.11 | 3.50 | 3.11 | |

Table 4: Ultimate analysis measurements given as wt. % as-determined basis.

| Name | Cycle | C | H | O | N | S | Total |
|-----------------------------|-------|-------|------|-------|------|------|-------|
| Residues | 1 | 49.63 | 6.52 | 41.87 | 0.49 | 0.04 | 98.55 |
| Stem wood | 2 | 48.89 | 6.53 | 44.12 | 0.18 | 0.01 | 99.73 |
| Bark | 3 | 51.84 | 6.14 | 40.97 | 0.34 | 0.02 | 99.31 |
| Needles | 4 | 50.22 | 6.22 | 38.77 | 0.92 | 0.09 | 96.22 |
| Bark + needles | 5 | 50.35 | 6.18 | 40.21 | 0.67 | 0.06 | 97.47 |
| Residues (rep 1) | 8 | 49.82 | 6.56 | 41.34 | 0.58 | 0.05 | 98.35 |
| Residues:bark:needles 1:1:1 | 10 | 50.58 | 6.31 | 40.43 | 0.59 | 0.05 | 97.96 |
| Residues:bark:needles 1:2:2 | 11 | 50.86 | 6.24 | 40.24 | 0.58 | 0.06 | 97.98 |
| Air classified (10 Hz) | 12 | 50.16 | 6.46 | 42.06 | 0.37 | 0.03 | 99.08 |
| Air classified (28 Hz) | 13 | 48.93 | 6.42 | 43.77 | 0.26 | 0.02 | 99.40 |
| Whole tree (13 yr) | 15 | 49.32 | 6.44 | 43.48 | 0.30 | 0.02 | 99.56 |
| Stem wood (13 yr) | 16 | 49.40 | 6.41 | 43.68 | 0.21 | 0.01 | 99.71 |
| Maximum difference | | 2.95 | 0.42 | 5.35 | 0.74 | 0.08 | |

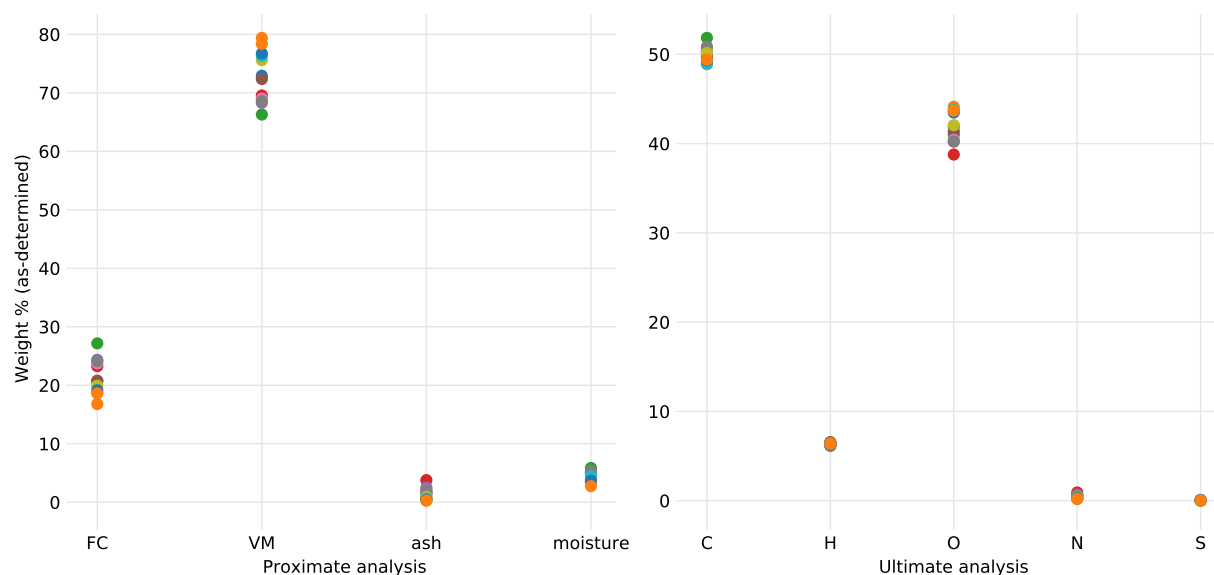


Figure 3: Comparison of proximate (left) and ultimate (right) analysis measurements for each feedstock. Values represent wt. % as-determined basis.

2.3 Feedstock chemical analysis

Chemical analysis data for each feedstock was supplied by the Idaho National Laboratory on a wt. % dry basis (D). A summary of the chemical analysis measurements is given in Tables 5 and 6. A comparison of the values are shown in Figure 4. The largest variations in the measured chemical fractions occur for the lignin and glucan with a maximum difference of 15 wt. % and 17.5 wt. % respectively.

Table 5: Chemical analysis measurements given as weight percent (wt. %) dry basis (D).

| Chemical component | Residues | Stem wood | Bark | Needles | Bark + needles | Residues (rep 1) |
|---------------------------|----------|-----------|--------|---------|----------------|------------------|
| structural inorganics | 0.94 | 0.32 | 0.5 | 3.23 | 1.76 | 1.24 |
| non-structural inorganics | 0.37 | 0 | 0.08 | 0.56 | 0.66 | 0.19 |
| water extractives | 4.91 | 2.76 | 2.9 | 5.95 | 4.01 | 6.18 |
| ethanol extractives | 0.62 | 0.31 | 0.46 | 1.35 | 0.98 | 0.68 |
| acetone extractives | 6.6 | 2.57 | 3.33 | 7.35 | 5.53 | 7.88 |
| lignin | 35.52 | 30.7 | 34.34 | 41.03 | 45.88 | 35.22 |
| glucan | 28.18 | 39.84 | 33.83 | 22.33 | 22.75 | 26.48 |
| xylan | 7.33 | 6.3 | 7.74 | 4.12 | 4.17 | 6.52 |
| galactan | 3.56 | 2.59 | 3.68 | 2.57 | 3.28 | 3.44 |
| arabinan | 1.93 | 0 | 3.5 | 1.52 | 2.4 | 2.84 |
| mannan | 7.64 | 14.94 | 9.15 | 7.44 | 5.35 | 6.33 |
| acetyl | 0.95 | 1.35 | 1.21 | 0.98 | 0.81 | 0.94 |
| total | 98.55 | 101.68 | 100.72 | 98.43 | 97.58 | 97.94 |

Table 6: Chemical analysis measurements given as weight percent (wt. %) dry basis (D).

| Chemical component | Residues:bark:needles 1:1:1 | Residues:bark:needles 1:2:2 | Air classified (10 Hz) | Air classified (28 Hz) | Whole tree (13 yr) | Stem wood (13 yr) |
|---------------------------|-----------------------------|-----------------------------|------------------------|------------------------|--------------------|-------------------|
| structural inorganics | 1.66 | 1.91 | 0.55 | 0.38 | 0.5 | 0.32 |
| non-structural inorganics | 0.02 | 0.21 | 0.31 | 0.22 | 0.08 | 0 |
| water extractives | 5.76 | 5.53 | 3.26 | 1.76 | 2.9 | 1.56 |
| ethanol extractives | 1.02 | 1.04 | 0.44 | 0.31 | 0.46 | 0.34 |
| acetone extractives | 6.87 | 6.51 | 4.02 | 2.4 | 3.33 | 1.76 |
| lignin | 42.06 | 42.9 | 35.11 | 35.23 | 33.34 | 33.4 |
| glucan | 23.37 | 22.92 | 31.99 | 34.37 | 33.83 | 38.15 |
| xylan | 5.07 | 4.64 | 7.63 | 8.39 | 7.74 | 7.97 |
| galactan | 2.95 | 3.03 | 3.63 | 3.9 | 3.68 | 3.63 |
| arabinan | 1.62 | 2.23 | 1.34 | 0 | 3.5 | 3.53 |
| mannan | 7.55 | 5.91 | 10.01 | 12.41 | 9.15 | 10.08 |
| acetyl | 0.9 | 0.85 | 1.18 | 1.24 | 1.21 | 1.41 |
| total | 98.85 | 97.68 | 99.47 | 100.61 | 99.72 | 102.15 |

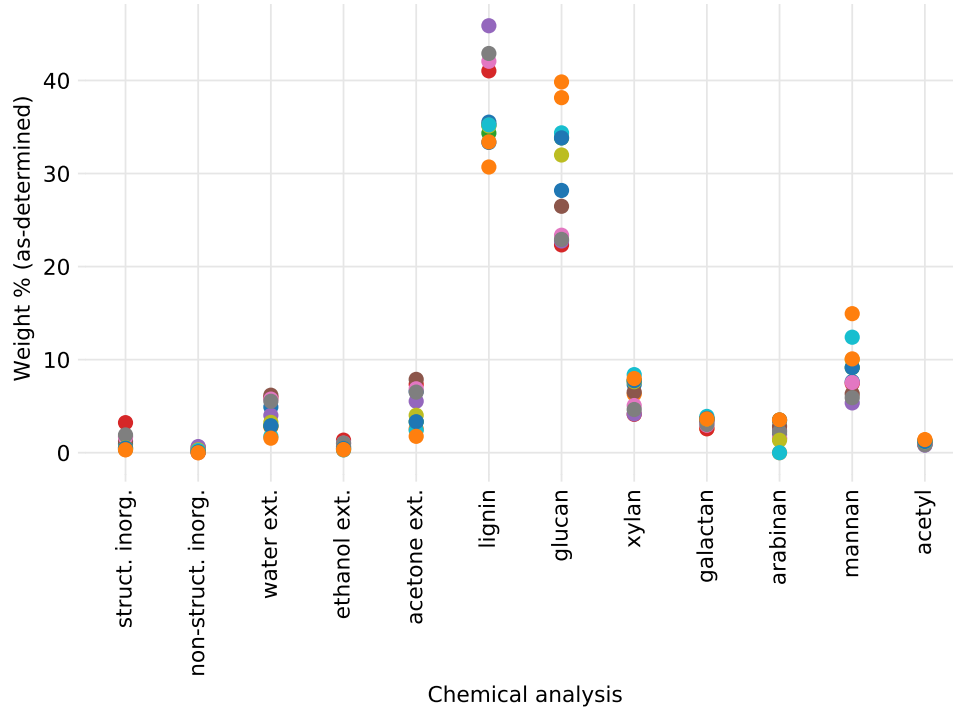


Figure 4: Comparison of chemical analysis measurements for each feedstock. FIXME: y-axis should be dry basis, not as-determined basis.

2.4 Bed particle characteristics

Characteristics of the sand particles that represent the fluidized bed material were obtained by NETL and are summarized in Table 7. A microscope image of the sand particles is shown in Figure 5. The particle density was determined from a helium pycnometer while size distribution and sphericity was obtained from QICPIC image analysis [6]. At the time of writing this report, bed particle characteristics were not utilized in the reactor models discussed in subsequent sections.

Table 7: Bed material (sand) characteristics.

| Parameter | Symbol | Value | Units |
|-------------------------------|--------|--------|-----------------|
| Particle envelope density | ρ | 2.7051 | g/cm^3 |
| Standard deviation of density | – | 0.0004 | g/cm^3 |
| Sauter mean diameter | SMD | 509 | μm |
| Average particle sphericity | ϕ | 0.874 | – |

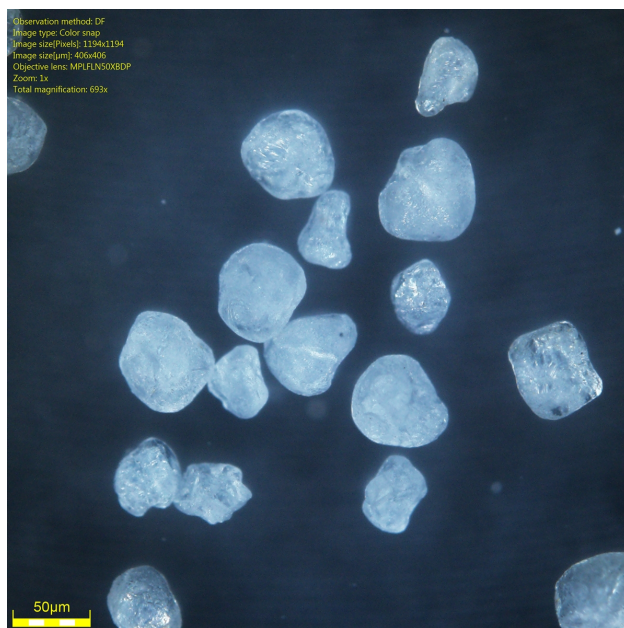


Figure 5: Microscope image of sand particles used for the bed material.

2.5 Product yields

Product yields measured from the fast pyrolysis of each feedstock in the fluidized bed reactor are given in Table 8. A comparison of the product yields from each feedstock is shown in Figure 6. The oil and char yields are the most variable between the different feedstocks while condensables and water vapor differ by a few percent.

Table 8: Measured reactor yields from each feedstock experiment. Values expressed as percent wet basis (w).

| Feedstock | Oil | Condensables | Light gas | Water vapor | Char | Total |
|-----------------------------|------|--------------|-----------|-------------|------|-------|
| Residues | 63.5 | 1.6 | 14.7 | 0.4 | 15.2 | 95.4 |
| Stem wood | 72.3 | 2.8 | 14.1 | 1.2 | 10.9 | 101.3 |
| Bark | 58.3 | 1.3 | 11.4 | 0.8 | 31.9 | 103.7 |
| Needles | 55.4 | 2.7 | 14.5 | 0.6 | 25.6 | 98.8 |
| Bark + needles | 55.5 | 1.3 | 15.1 | 1.2 | 16.5 | 89.6 |
| Residues (rep 1) | 62.6 | 2.5 | 15.9 | 2.5 | 17.3 | 100.8 |
| Residues:bark:needles 1:1:1 | 58.3 | 3.1 | 14.3 | 0.7 | 24.6 | 101.0 |
| Residues:bark:needles 1:2:2 | 57.1 | 0.6 | 15.0 | 2.0 | 25.0 | 99.7 |
| Air classified (10 Hz) | 57.6 | 3.0 | 16.2 | 3.2 | 16.3 | 96.3 |
| Air classified (28 Hz) | 65.0 | 2.5 | 17.9 | 1.6 | 13.9 | 100.9 |
| Whole tree (13 yr) | 63.1 | 1.8 | 17.7 | 2.1 | 13.9 | 98.6 |
| Stem wood (13 yr) | 67.8 | 1.9 | 15.2 | 3.2 | 12.2 | 100.3 |

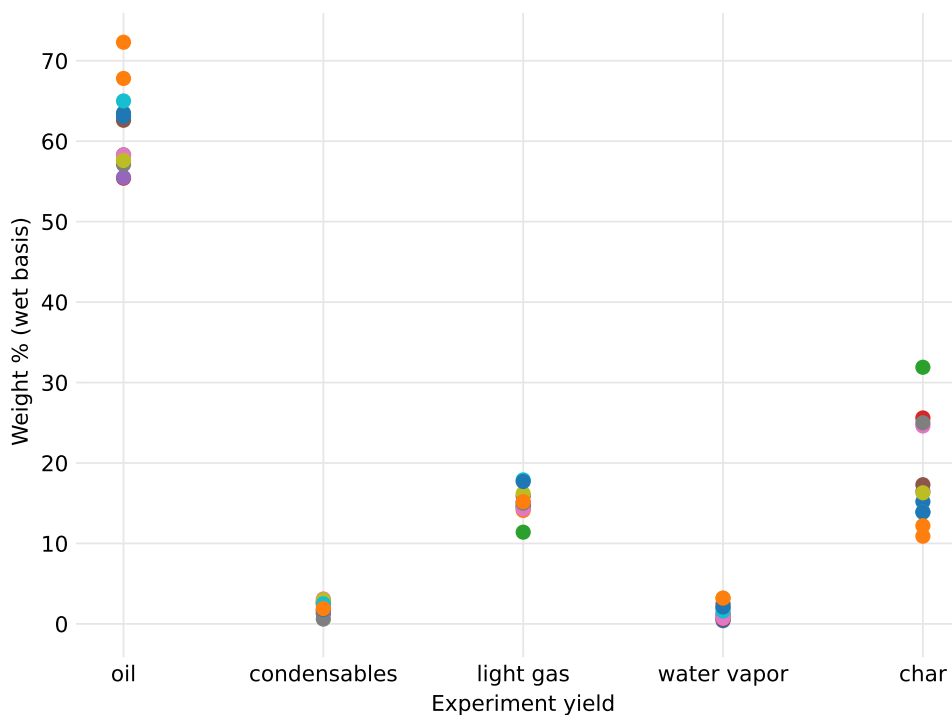


Figure 6: Comparison of the measured product yields for each feedstock. Values shown as percent wet basis.

3 Model development

This section presents the equations used to convert the measured data to different bases for use in the reactor models. The biomass pyrolysis kinetics scheme along with the associated biomass characterization method is also detailed. Finally, the reduced-order batch and continuous stirred tank reactor (CSTR) models are presented.

3.1 Basis of analysis

The proximate analysis data was converted to different bases using ASTM methods [1]. Equations 1–4 convert the as-determined (ad) basis to as-received (ar), dry (d), and dry ash-free (daf) bases where X is the wt. % of the corresponding basis value, M is the moisture content, and ADL is the air-dry loss assumed to be 22 wt. %. As an example, to obtain the as-received value of the fixed carbon use $FC_{ar} = FC_{ad} \times \frac{100-M_{ar}}{100-M_{ad}}$.

$$M_{ar} = \left(M_{ad} \times \frac{100 - ADL}{100} \right) + ADL \quad (1)$$

$$X_{ar} = X_{ad} \times \frac{100 - M_{ar}}{100 - M_{ad}} \quad (2)$$

$$X_d = X_{ad} \times \frac{100}{100 - M_{ad}} \quad (3)$$

$$X_{daf} = X_{ad} \times \frac{100}{100 - M_{ad} - ash_{ad}} \quad (4)$$

Similarly, the ultimate analysis data was also converted to different bases using the ASTM methods [1]. Equations 1–4 convert the carbon, nitrogen, and sulfur fractions to different bases while Equations 5–8 are for the hydrogen and oxygen fractions. Equation 9 calculates the CHO basis from the dry ash-free basis.

$$H_{ar} = (H_{ad} - 0.1119 M_{ad}) \times \frac{100 - M_{ar}}{100 - M_{ad}} \quad (5)$$

$$O_{ar} = (O_{ad} - 0.8881 M_{ad}) \times \frac{100 - M_{ar}}{100 - M_{ad}} \quad (6)$$

$$H_d = (H_{ad} - 0.1119 M_{ad}) \times \frac{100}{100 - M_{ad}} \quad (7)$$

$$O_d = (O_{ad} - 0.8881 M_{ad}) \times \frac{100}{100 - M_{ad}} \quad (8)$$

$$X_{cho} = X_{daf} \times \frac{100}{100 - N_{daf} - S_{daf}} \quad (9)$$

For the chemical analysis data, the given dry basis values P_d are converted to a dry ash-free basis P_{daf} using Equation 10 where P_{struct} is the structural inorganics, $P_{nonstruct}$ is the non-structural inorganics, and $P_{d,total}$ is the sum of the dry basis values.

$$P_{daf} = P_d \times \frac{100}{P_{d,total} - P_{struct} - P_{nonstruct}} \quad (10)$$

3.2 Biomass pyrolysis kinetics

The kinetic reaction mechanisms presented in the Debiagi et al. 2018 paper [2] were used to model biomass pyrolysis in the fluidized bed reactor. Table 9 summarizes the reactions along with the associated prefactors and activation energies. A description of the chemical species in the Debiagi et al. kinetic scheme is provided in Table 10.

Table 9: Kinetic reactions for biomass pyrolysis where A is the prefactor, E is the activation energy, and T is temperature. Source [2].

| Item | Reaction | A (1/s) | E (cal/mol) |
|------|---|-------------------------------|-------------|
| 1 | CELL → CELLA | 1.5×10^{14} | 47,000 |
| 2 | CELLA → 0.40 CH ₂ OHCHO + 0.03 CHOCHO + 0.17 CH ₃ CHO + 0.25 C ₆ H ₆ O ₃ + 0.35 C ₂ H ₅ CHO + 0.20 CH ₃ OH + 0.15 CH ₂ O + 0.49 CO + 0.05 G{CO} + 0.43 CO ₂ + 0.13 H ₂ + 0.93 H ₂ O + 0.05 G{COH ₂ } loose + 0.02 HCOOH + 0.05 CH ₂ OHCH ₂ CHO + 0.05 CH ₄ + 0.1 G{H ₂ } + 0.66 CHAR | 2.5×10^6 | 19,100 |
| 3 | CELLA → C ₆ H ₁₀ O ₅ | $3.3 \times T$ | 10,000 |
| 4 | CELL → 4.45 H ₂ O + 5.45 CHAR + 0.12 G{COH ₂ } stiff + 0.18 G{COH ₂ } loose + 0.25 G{CO} + 0.125 G{H ₂ } + 0.125 H ₂ | 9.0×10^7 | 31,000 |
| 5 | GMSW → 0.70 HCE1 + 0.30 HCE2 | 1.0×10^{10} | 31,000 |
| 6 | XYHW → 0.35 HCE1 + 0.65 HCE2 | 1.25×10^{11} | 31,400 |
| 7 | XYGR → 0.12 HCE1 + 0.88 HCE2 | 1.25×10^{11} | 30,000 |
| 8 | HCE1 → 0.25 C ₅ H ₈ O ₄ + 0.25 C ₆ H ₁₀ O ₅ + 0.16 FURFURAL + 0.13 C ₆ H ₆ O ₃ + 0.09 CO ₂ + 0.1 CH ₄ + 0.54 H ₂ O + 0.06 CH ₂ OHCH ₂ CHO + 0.1 CHOCHO + 0.02 H ₂ + 0.1 CHAR | $16.0 \times T$ | 12,900 |
| 9 | HCE1 → 0.4 H ₂ O + 0.39 CO ₂ + 0.05 HCOOH + 0.49 CO + 0.01 G{CO} + 0.51 G{CO ₂ } + 0.05 G{H ₂ } + 0.4 CH ₂ O + 0.43 G{COH ₂ } loose + 0.3 CH ₄ + 0.325 G{CH ₄ } + 0.1 C ₂ H ₄ + 0.075 G{C ₂ H ₄ } + 0.975 CHAR + 0.37 G{COH ₂ } stiff + 0.1 H ₂ + 0.2 G{C ₂ H ₆ } | $3.0 \times 10^{-3} \times T$ | 3,600 |
| 10 | HCE2 → 0.3 CO + 0.5125 CO ₂ + 0.1895 CH ₄ + 0.5505 H ₂ + 0.056 H ₂ O + 0.049 C ₂ H ₅ OH + 0.035 CH ₂ OHCHO + 0.105 CH ₃ CO ₂ H + 0.0175 HCOOH + 0.145 FURFURAL + 0.05 G{CH ₄ } + 0.105 G{CH ₃ OH} + 0.1 G{C ₂ H ₄ } + 0.45 G{CO ₂ } + 0.18 G{COH ₂ } loose + 0.7125 CHAR + 0.21 G{H ₂ } + 0.78 G{COH ₂ } stiff + 0.2 G{C ₂ H ₆ } | 7.0×10^9 | 30,500 |
| 11 | LIGH → LIGOH + 0.5 C ₂ H ₅ CHO + 0.4 C ₂ H ₄ + 0.2 CH ₂ OHCHO + 0.1 CO + 0.1 C ₂ H ₆ | 6.7×10^{12} | 37,500 |
| 12 | LIGO → LIGOH + CO ₂ | 3.3×10^8 | 25,500 |
| 13 | LIGC → 0.35 LIGCC + 0.1 VANILLIN + 0.1 C ₆ H ₅ OCH ₃ + 0.27 C ₂ H ₄ + H ₂ O + 0.17 G{COH ₂ } loose + 0.4 G{COH ₂ } stiff + 0.22 CH ₂ O + 0.21 CO + 0.1 CO ₂ + 0.36 G{CH ₄ } + 5.85 CHAR + 0.2 G{C ₂ H ₆ } + 0.1 G{H ₂ } | 1.0×10^{11} | 37,200 |
| 14 | LIGCC → 0.25 VANILLIN + 0.15 CRESOL + 0.15 C ₆ H ₅ OCH ₃ + 0.35 CH ₂ OHCHO + 0.7 H ₂ O + 0.45 CH ₄ + 0.3 C ₂ H ₄ + 0.7 H ₂ + 1.15 CO + 0.4 G{CO} + 6.80 CHAR + 0.4 C ₂ H ₆ | 1.0×10^4 | 24,800 |
| 15 | LIGOH → 0.9 LIG + H ₂ O + 0.1 CH ₄ + 0.6 CH ₃ OH + 0.3 G{CH ₃ OH} + 0.05 CO ₂ + 0.65 CO + 0.6 G{CO} + 0.05 HCOOH + 0.45 G{COH ₂ } loose + 0.4 G{COH ₂ } stiff + 0.25 G{CH ₄ } + 0.1 G{C ₂ H ₄ } + 0.15 G{C ₂ H ₆ } + 4.25 CHAR + 0.025 C ₂ H ₂ O ₄ + 0.1 C ₂ H ₃ CHO | 1.5×10^8 | 30,000 |
| 16 | LIG → VANILLIN + 0.1 C ₆ H ₅ OCH ₃ + 0.5 C ₂ H ₄ + 0.6 CO + 0.3 CH ₃ CHO + 0.1 CHAR | $4.0 \times T$ | 12,000 |

| | | | |
|----|---|-------------------------------|--------|
| 17 | LIG \rightarrow 0.6 H ₂ O + 0.3 CO + 0.1 CO ₂ + 0.2 CH ₄ + 0.4 CH ₂ O + 0.2 G{CO} + 0.4 G{CH ₄ } + 0.5 G{C ₂ H ₄ } + 0.4 G{CH ₃ OH} + 1.25 G{COH ₂ } loose + 0.65 G{COH ₂ } stiff + 6.1 CHAR + 0.1 G{H ₂ } | $8.3 \times 10^{-2} \times T$ | 8,000 |
| 18 | LIG \rightarrow 0.6 H ₂ O + 2.6 CO + 0.6 CH ₄ + 0.4 CH ₂ O + 0.75 C ₂ H ₄ + 0.4 CH ₃ OH + 4.5 CHAR + 0.5 C ₂ H ₆ | 1.5×10^9 | 31,500 |
| 19 | TGL \rightarrow C ₂ H ₃ CHO + 2.5 MLINO + 0.5 U2ME12 | 7.0×10^{12} | 45,700 |
| 20 | TANN \rightarrow 0.85 C ₆ H ₅ OH + 0.15 G{C ₆ H ₅ OH} + G{CO} + H ₂ O + ITANN | 2.0×10^1 | 10,000 |
| 21 | ITANN \rightarrow 5 CHAR + 2 CO + H ₂ O + 0.55 G{COH ₂ } loose + 0.45 G{COH ₂ } stiff | 1.0×10^3 | 25,000 |
| 22 | G{CO ₂ } \rightarrow CO ₂ | 1.0×10^6 | 24,500 |
| 23 | G{CO} \rightarrow CO | 5.0×10^{12} | 52,500 |
| 24 | G{CH ₃ OH} \rightarrow CH ₃ OH | 2.0×10^{12} | 50,000 |
| 25 | G{COH ₂ }loose \rightarrow 0.2 CO + 0.2 H ₂ + 0.8 H ₂ O + 0.8 CHAR | 6.0×10^{10} | 50,000 |
| 26 | G{C ₂ H ₆ } \rightarrow C ₂ H ₆ | 1.0×10^{11} | 52,000 |
| 27 | G{CH ₄ } \rightarrow CH ₄ | 1.0×10^{11} | 53,000 |
| 28 | G{C ₂ H ₄ } \rightarrow C ₂ H ₄ | 1.0×10^{11} | 54,000 |
| 29 | G{C ₆ H ₅ OH} \rightarrow C ₆ H ₅ OH | 1.5×10^{12} | 55,000 |
| 30 | G{COH ₂ }stiff \rightarrow 0.8 CO + 0.8 H ₂ + 0.2 H ₂ O + 0.2 CHAR | 1.0×10^9 | 59,000 |
| 31 | G{H ₂ } \rightarrow H ₂ | 1.0×10^8 | 70,000 |
| 32 | ACQUA \rightarrow H ₂ O | $1.0 \times T$ | 8,000 |

Table 10: Description of the chemical species in the Debiagi kinetics scheme for biomass pyrolysis. Source [2].

| Item | Name | Formula | Phase | Description |
|------|-----------------------------------|---|-------------|----------------------------|
| 1 | CELL | C ₆ H ₁₀ O ₅ | solid | cellulose |
| 2 | CELLA | C ₆ H ₁₀ O ₅ | solid | active cellulose |
| 3 | GMSW | C ₅ H ₈ O ₄ | solid | hemicellulose softwood |
| 4 | XYHW | C ₅ H ₈ O ₄ | solid | hemicellulose hardwood |
| 5 | XYGR | C ₅ H ₈ O ₄ | solid | hemicellulose grass |
| 6 | HCE1 | C ₅ H ₈ O ₄ | solid | intermediate hemicellulose |
| 7 | HCE2 | C ₅ H ₈ O ₄ | solid | intermediate hemicellulose |
| 8 | ITANN | C ₈ H ₄ O ₄ | solid | intermediate phenolics |
| 9 | LIG | C ₁₁ H ₁₂ O ₄ | solid | intermediate lignin |
| 10 | LIGC | C ₁₅ H ₁₄ O ₄ | solid | carbon rich lignin |
| 11 | LIGCC | C ₁₅ H ₁₄ O ₄ | solid | intermediate lignin |
| 12 | LIGH | C ₂₂ H ₂₈ O ₉ | solid | hydrogen rich lignin |
| 13 | LIGO | C ₂₀ H ₂₂ O ₁₀ | solid | oxygen rich lignin |
| 14 | LIGOH | C ₁₉ H ₂₂ O ₈ | solid | intermediate lignin |
| 15 | TANN | C ₁₅ H ₁₂ O ₇ | solid | tannins |
| 16 | TGL | C ₅₇ H ₁₀₀ O ₇ | solid | triglycerides |
| 17 | CHAR | C | solid | char as pure carbon |
| 18 | ACQUA | H ₂ O | solid | biomass moisture content |
| 19 | G{COH ₂ } loose | CH ₂ O | metaplastic | loose formaldehyde |
| 20 | G{CO ₂ } | CO ₂ | metaplastic | trapped carbon dioxide |
| 21 | G{CO} | CO | metaplastic | trapped carbon monoxide |
| 22 | G{CH ₃ OH} | CH ₄ O | metaplastic | trapped methanol |
| 23 | G{CH ₄ } | CH ₄ | metaplastic | trapped methane |
| 24 | G{C ₂ H ₄ } | C ₂ H ₄ | metaplastic | trapped ethylene |

| | | | | |
|----|---------------|--|-------------|-------------------------------|
| 25 | G{C6H5OH} | C ₆ H ₆ O | metaplastic | trapped phenol |
| 26 | G{COH2} stiff | CH ₂ O | metaplastic | stiff formaldehyde |
| 27 | G{H2} | H ₂ | metaplastic | trapped hydrogen |
| 28 | G{C2H6} | C ₂ H ₆ | metaplastic | trapped ethane |
| 29 | C2H4 | C ₂ H ₄ | gas | ethylene |
| 30 | C2H6 | C ₂ H ₆ | gas | ethane |
| 31 | CH2O | CH ₂ O | gas | formaldehyde |
| 32 | CH4 | CH ₄ | gas | methane |
| 33 | CO | CO | gas | carbon monoxide |
| 34 | CO2 | CO ₂ | gas | carbon dioxide |
| 35 | H2 | H ₂ | gas | hydrogen |
| 36 | C2H3CHO | C ₃ H ₄ O | liquid | acrolein |
| 37 | C2H5CHO | C ₃ H ₆ O | liquid | propionaldehyde |
| 38 | C2H5OH | C ₂ H ₆ O | liquid | ethanol |
| 39 | C5H8O4 | C ₅ H ₈ O ₄ | liquid | xylofuranose |
| 40 | C6H10O5 | C ₆ H ₁₀ O ₅ | liquid | levoglucosan |
| 41 | C6H5OCH3 | C ₇ H ₈ O | liquid | anisole |
| 42 | C6H5OH | C ₆ H ₆ O | liquid | phenol |
| 43 | C6H6O3 | C ₆ H ₆ O ₃ | liquid | hydroxymethylfurfural |
| 44 | C24H28O4 | C ₂₄ H ₂₈ O ₄ | liquid | heavy molecular weight lignin |
| 45 | CH2OHCH2CHO | C ₃ H ₆ O ₂ | liquid | propionic acid |
| 46 | CH2OHCHO | C ₂ H ₄ O ₂ | liquid | acetic acid |
| 47 | CH3CHO | C ₂ H ₄ O | liquid | acetaldehyde |
| 48 | CH3CO2H | C ₂ H ₄ O ₂ | liquid | acetic acid |
| 49 | CH3OH | CH ₄ O | liquid | methanol |
| 50 | CHOCHO | C ₂ H ₂ O ₂ | liquid | glyoxal |
| 51 | CRESOL | C ₇ H ₈ O | liquid | cresol |
| 52 | FURFURAL | C ₅ H ₄ O ₂ | liquid | 2-furaldehyde |
| 53 | H2O | H ₂ O | liquid | water from reactions |
| 54 | HCOOH | CH ₂ O ₂ | liquid | formic acid |
| 55 | MLINO | C ₁₉ H ₃₄ O ₂ | liquid | methyl linoleate |
| 56 | U2ME12 | C ₁₃ H ₂₂ O ₂ | liquid | linalyl propionate |
| 57 | VANILLIN | C ₈ H ₈ O ₃ | liquid | vanillin |

The Debiagi kinetics rely on an initial biomass composition defined as cellulose (CELL), hemicellulose (HCELL), carbon-rich lignin (LIGC), hydrogen-rich lignin (LIGH), oxygen-rich lignin (LIGO), tannins (TANN), and triglycerides (TGL). The hemicellulose reaction mechanisms consider different types of biomass such as softwood (GMSW), hardwood (XYHW), and grass (XYGR) feedstocks. Products generated from the biomass pyrolysis are grouped into solid, metaplastic, gas, and liquid phases. Solid and metaplastic species are combined and compared to the NREL reactor's char yield. All liquid species are combined and compared to the reactor's total liquid yield. Figure 7 illustrates the conversion of the biomass components to pyrolysis products of liquids, solids, metaplastics, and gases as discussed in the Debiagi et al. kinetics scheme.

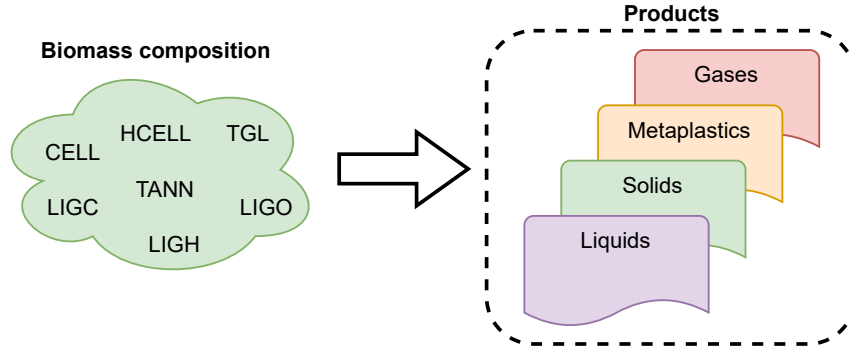


Figure 7: Seven biomass components convert to pyrolysis products according to the Debiagi et al. biomass pyrolysis kinetics scheme.

3.3 Biomass composition

According to the Debiagi et al. 2015 paper [3], the chemical components of the biomass are defined as shown in Table 11. The Debiagi paper does not provide information on how to experimentally determine these components. However, the paper provides a characterization method which estimates the biomass composition based on elemental (ultimate) analysis data. The characterization method uses the carbon (C) and hydrogen (H) content of the biomass to predict the biochemical composition in terms of cellulose, hemicellulose, lignin, tannins, and triglycerides. Splitting parameters α , β , γ , δ , and ϵ are used to improve the validity of the characterization procedure by accounting for extractives in the biomass.

Table 11: Chemical components representing biomass composition needed for the Debiagi et al. pyrolysis kinetics.

| Biomass composition | Symbol | Description |
|---------------------|----------------------|--|
| cellulose | CELL | glucan |
| hemicellulose | GMSW XYHW XYGR | mixture of sugars such as hexoses and pentoses; mainly xylose, mannose, galactose, and arabinose |
| lignin | LIG | aromatic alcohols such as coniferyl, sinapyl, p-coumaryl alcohol |
| lignin-c | LIG-C | carbon-rich lignin |
| lignin-h | LIG-H | hydrogen-rich lignin |
| lignin-o | LIG-O | oxygen-rich lignin |
| tannins | TANN | hydrophilic extractives, phenolics, ethanol and water, represented by a galocatechin polymer |
| triglycerides | TGL | hydrophobic extractives, hexane and ether, linoleic acid |

As discussed previously, the largest differences in the chemical analysis feedstock data are for the lignin, glucan, and mannan fractions. These fractions represent the cellulose (glucan), hemicellulose (xylan, galactan, arabinan, mannan, acetyl), and total lignin components of the biomass composition. Unfortunately, the chemical analysis data does not directly relate to all the biomass components needed for the pyrolysis kinetics.

Using the C and H values from the ultimate analysis CHO basis and default values for the splitting parameters, the biomass composition is estimated using the characterization method from Debiagi et al. The estimated cellulose, hemicellulose, and total lignin (LIGC + LIGH + LIGO) values are compared to the chemical analysis measurements using

$$f(x) = (cell_{est} - cell_{meas})^2 + (hemi_{est} - hemi_{meas})^2 + (lignin_{est} - lignin_{meas})^2 \quad (11)$$

where f is the function to be minimized, $cell_{est}$ is the estimated cellulose, $cell_{meas}$ is the cellulose from chemical analysis, $hemi_{est}$ is the estimated hemicellulose, $hemi_{meas}$ is the hemicellulose from chemical analysis, $lignin_{est}$ is the estimated lignin, and $lignin_{meas}$ is the lignin from chemical analysis. The L-BFGS-B algorithm is applied to the minimization function to generate the optimum splitting parameter values such that the cellulose, hemicellulose, and total lignin are similar to the values obtained from the chemical analysis data. Figure 8 demonstrates the biomass composition minimization procedure.

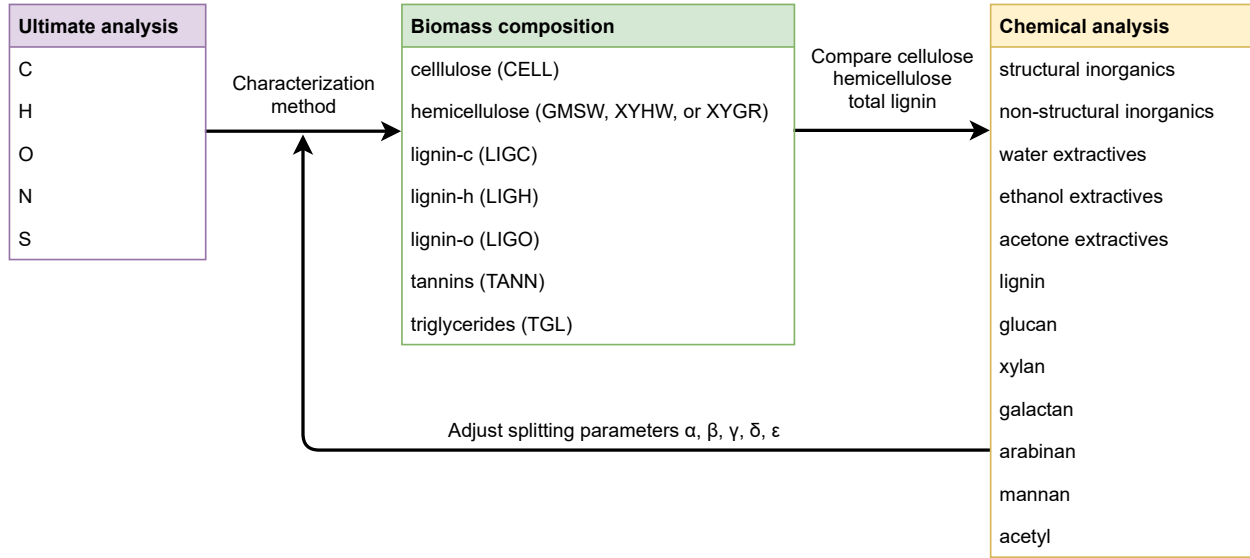


Figure 8: Biomass composition determined from ultimate analysis data and compared with measured chemical analysis data for cellulose, hemicellulose, and total lignin.

3.4 Batch reactor and CSTR models

The material balance for a chemical reactor considers the inlet and outlet flows of the system along with accumulation and reaction effects

$$\text{accumulation} = \text{input} - \text{output} + \text{reaction}$$

$$\frac{dC_A}{dt} V = vC_{A0} - vC_A + r_A V \quad (12)$$

where A represents a chemical species, C_A is the outlet concentration (mol/m^3), C_{A0} is the inlet concentration (mol/m^3), V is the reactor volume (m^3), v is the volumetric flow rate (m^3/s), and r_A is the reaction rate ($\text{mol}/\text{m}^3\text{s}$). The reaction rate is determined by multiplying a forward rate constant k by the concentration in the tank. The rate constant is calculated from an Arrhenius function

$$k = A T^b e^{-E/RT} \quad (13)$$

where A is the pre-exponential factor, T is the reaction temperature, b is the temperature exponent, E is the activation energy, and R is the universal gas constant.

A batch reactor was modeled to understand the time scales associated with the biomass pyrolysis kinetics. For a batch reactor, input and output is zero therefore only the accumulation and reaction terms remain in the material balance. For a constant volume reactor the V terms cancel out resulting in the following material balance for a batch reactor model

$$\text{accumulation} = 0 - 0 + \text{reaction}$$

$$\frac{dC_A}{dt} = r_A \quad (14)$$

A depiction of a batch reactor can be seen in Figure 9. The Cantera Python package was used to model the batch reactor as an IdealGasReactor [5].

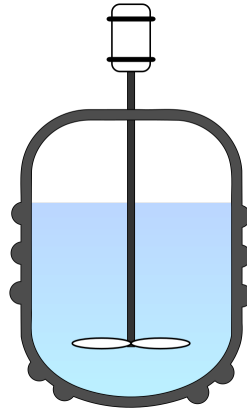


Figure 9: Representation of a batch reactor system. Source: Wikipedia.

To account for inlet and outlet flows, a continuous stirred tank reactor (CSTR) system at steady-state conditions was also modeled. The material balance for a steady-state CSTR does not account for accumulation but does consider the residence time in the system

$$\begin{aligned}
 0 &= \text{input} - \text{output} + \text{reaction} \\
 0 &= vC_{A0} - vC_A + r_A V \\
 C_A &= C_{A0} + r_A \tau
 \end{aligned} \tag{15}$$

where τ is the residence time (s) of chemical A in the reactor. A depiction of a CSTR system with its inlet and outlet flows is shown in Figure 10. The Cantera Python package was used to model the CSTR using an IdealGasReactor with inlet and outlet flows [5].

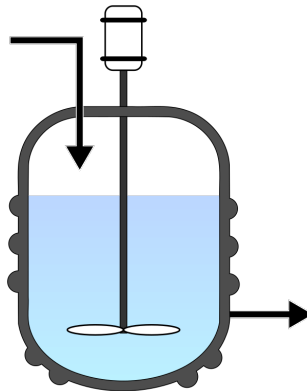


Figure 10: Representation of a continuous stirred-tank reactor (CSTR) system with inlet and outlet flows. Source: Wikipedia.

A series of continuous stirred-tank reactor (CSTR) models were used to model the mixing (residence time) of the different feedstocks in the NREL fluidized bed reactor. The residence time for each feedstock was obtained from CFD simulations performed by

NETL. As the number of CSTRs increases, the reactor model behaves more like a plug flow reactor (PFR). The modeling technique is illustrated by Figure 11 where the N subscript represents the total number of CSTRs.



Figure 11: Depiction of a bubbling fluidized bed reactor modeled as a series of CSTRs.

To exclude the nitrogen gas fraction from the calculated CSTR product yields, the mass fractions are converted from a N_2 basis to a N_2 free basis

$$Y_{i,N_2 free} = \frac{Y_{i,N_2}}{Y_{gas,N_2} + Y_{liquid,N_2} + Y_{solid,N_2} + Y_{metaplastic,N_2} - Y_{N_2}} \quad (16)$$

where Y is the mass fraction, and i represents the gas, liquid, solid, and metaplastic phases.

4 Results and discussion

Feedstock characterization, batch reactor, and CSTR model results are discussed in this section.

4.1 Feedstock characterization

Table 12 presents the proximate and ultimate analysis data on an as-determined (AD), as-received (AR), dry (D), dry ash-free (DAF), and CHO basis. The reported H and O for the ultimate analysis data does not include the H and O in the moisture; therefore, the total value for the as-determined basis (AD column) excludes the moisture percentage.

Table 12: Proximate and ultimate analysis basis values for each feedstock given as wt. %.
Reported H and O values for ultimate analysis AD basis excludes H and O in moisture.

| Residues | AD | AR | D | DAF | CHO |
|------------------|--------|--------|--------|--------|--------|
| FC | 20.72 | 17.33 | 21.79 | 22.13 | – |
| VM | 72.92 | 60.99 | 76.69 | 77.88 | – |
| ash | 1.45 | 1.21 | 1.53 | – | – |
| moisture | 4.92 | 20.58 | – | – | – |
| total | 100.01 | 100.01 | 100.01 | 100.01 | – |
| C | 49.63 | 38.71 | 52.20 | 53.01 | 53.31 |
| H | 6.52 | 4.66 | 6.28 | 6.38 | 6.41 |
| O | 41.87 | 29.25 | 39.44 | 40.05 | 40.28 |
| N | 0.49 | 0.38 | 0.52 | 0.52 | – |
| S | 0.04 | 0.03 | 0.04 | 0.04 | – |
| ash | 1.45 | 1.13 | 1.53 | – | – |
| moisture | (4.92) | 25.84 | – | – | – |
| total | 100 | 100 | 100 | 100 | 100 |
| Stem wood | AD | AR | D | DAF | CHO |
| FC | 16.79 | 13.10 | 17.41 | 17.46 | – |
| VM | 79.40 | 61.93 | 82.32 | 82.56 | – |
| ash | 0.28 | 0.22 | 0.29 | – | – |
| moisture | 3.55 | 24.77 | – | – | – |
| total | 100.02 | 100.02 | 100.02 | 100.02 | – |
| C | 48.89 | 38.13 | 50.69 | 50.84 | 50.94 |
| H | 6.53 | 4.78 | 6.36 | 6.38 | 6.39 |
| O | 44.12 | 31.95 | 42.48 | 42.60 | 42.68 |
| N | 0.18 | 0.14 | 0.19 | 0.19 | – |
| S | 0.01 | 0.01 | 0.01 | 0.01 | – |
| ash | 0.28 | 0.22 | 0.29 | – | – |
| moisture | (3.55) | 24.77 | – | – | – |
| total | 100.01 | 100.01 | 100.01 | 100.01 | 100.01 |
| Bark | AD | AR | D | DAF | CHO |
| FC | 27.16 | 21.18 | 28.85 | 29.07 | – |
| VM | 66.29 | 51.71 | 70.42 | 70.94 | – |
| ash | 0.70 | 0.55 | 0.74 | – | – |
| moisture | 5.86 | 26.57 | – | – | – |
| total | 100.01 | 100.01 | 100.01 | 100.01 | – |

| | | | | | |
|-------------------------|--------|--------|--------|--------|--------|
| C | 51.84 | 40.44 | 55.07 | 55.48 | 55.69 |
| H | 6.14 | 4.28 | 5.83 | 5.87 | 5.89 |
| O | 40.97 | 27.90 | 37.99 | 38.28 | 38.42 |
| N | 0.34 | 0.27 | 0.36 | 0.36 | – |
| S | 0.02 | 0.02 | 0.02 | 0.02 | – |
| ash | 0.70 | 0.55 | 0.74 | – | – |
| moisture | (5.86) | 26.57 | – | – | – |
| total | 100.01 | 100.01 | 100.01 | 100.01 | 100.01 |
| Needles | AD | AR | D | DAF | CHO |
| FC | 23.26 | 18.14 | 24.08 | 25.06 | – |
| VM | 69.54 | 54.24 | 72.00 | 74.94 | – |
| ash | 3.78 | 2.95 | 3.91 | – | – |
| moisture | 3.42 | 24.67 | – | – | – |
| total | 100 | 100 | 100 | 100 | – |
| C | 50.22 | 39.17 | 52.00 | 54.12 | 54.71 |
| H | 6.22 | 4.55 | 6.04 | 6.29 | 6.36 |
| O | 38.77 | 27.87 | 37.00 | 38.51 | 38.93 |
| N | 0.92 | 0.72 | 0.95 | 0.99 | – |
| S | 0.09 | 0.07 | 0.09 | 0.10 | – |
| ash | 3.78 | 2.95 | 3.91 | – | – |
| moisture | (3.42) | 24.67 | – | – | – |
| total | 100 | 100 | 100 | 100 | 100 |
| Bark + needles | AD | AR | D | DAF | CHO |
| FC | 24.35 | 18.99 | 25.59 | 26.29 | – |
| VM | 68.30 | 53.27 | 71.78 | 73.73 | – |
| ash | 2.52 | 1.97 | 2.65 | – | – |
| moisture | 4.85 | 25.78 | – | – | – |
| total | 100.02 | 100.02 | 100.02 | 10.02 | – |
| C | 50.35 | 39.27 | 52.92 | 54.36 | 54.79 |
| H | 6.18 | 4.40 | 5.92 | 6.09 | 6.13 |
| O | 40.21 | 28.00 | 37.73 | 38.76 | 39.07 |
| N | 0.67 | 0.52 | 0.70 | 0.72 | – |
| S | 0.06 | 0.05 | 0.06 | 0.06 | – |
| ash | 2.52 | 1.97 | 2.65 | – | – |
| moisture | (4.85) | 25.78 | – | – | – |
| total | 99.99 | 99.99 | 99.99 | 99.99 | 99.99 |
| Residues (rep 1) | AD | AR | D | DAF | CHO |

| | | | | | |
|------------------------------------|-----------|-----------|----------|------------|------------|
| FC | 20.78 | 16.21 | 21.92 | 22.31 | – |
| VM | 72.37 | 56.45 | 76.34 | 77.69 | – |
| ash | 1.65 | 1.29 | 1.74 | – | – |
| moisture | 5.20 | 26.06 | – | – | – |
| total | 100 | 100 | 100 | 100 | – |
| C | 49.82 | 38.86 | 52.55 | 53.48 | 53.85 |
| H | 6.56 | 4.66 | 6.31 | 6.42 | 6.46 |
| O | 41.34 | 28.64 | 38.74 | 39.42 | 39.69 |
| N | 0.58 | 0.45 | 0.61 | 0.62 | – |
| S | 0.05 | 0.04 | 0.05 | 0.05 | – |
| ash | 1.65 | 1.29 | 1.74 | – | – |
| moisture | (5.20) | 26.06 | – | – | – |
| total | 100 | 100 | 100 | 100 | 100 |
| Residues:bark:needles 1:1:1 | AD | AR | D | DAF | CHO |
| FC | 23.75 | 18.52 | 25.05 | 25.60 | – |
| VM | 69.02 | 53.84 | 72.80 | 74.41 | – |
| ash | 2.05 | 1.60 | 2.16 | – | – |
| moisture | 5.19 | 26.05 | – | – | – |
| total | 100.01 | 100.01 | 100.01 | 100.01 | – |
| C | 50.58 | 39.45 | 53.35 | 54.53 | 54.91 |
| H | 6.31 | 4.47 | 6.04 | 6.18 | 6.22 |
| O | 40.43 | 27.94 | 37.78 | 38.62 | 38.88 |
| N | 0.59 | 0.46 | 0.62 | 0.64 | – |
| S | 0.05 | 0.04 | 0.05 | 0.05 | – |
| ash | 2.05 | 1.60 | 2.16 | – | – |
| moisture | (5.19) | 26.05 | – | – | – |
| total | 100.01 | 100.01 | 100.01 | 100.01 | 100.01 |
| Residues:bark:needles 1:2:2 | AD | AR | D | DAF | CHO |
| FC | 24.12 | 18.81 | 25.47 | 26.02 | – |
| VM | 68.57 | 53.48 | 72.40 | 73.98 | – |
| ash | 2.02 | 1.58 | 2.13 | – | – |
| moisture | 5.29 | 26.13 | – | – | – |
| total | 100 | 100 | 100 | 100 | – |
| C | 50.86 | 39.67 | 53.70 | 54.87 | 55.25 |
| H | 6.24 | 4.41 | 5.96 | 6.09 | 6.14 |
| O | 40.24 | 27.72 | 37.53 | 38.34 | 38.61 |

| | | | | | |
|-----------------------------|-----------|-----------|----------|------------|------------|
| N | 0.58 | 0.45 | 0.61 | 0.63 | – |
| S | 0.06 | 0.05 | 0.06 | 0.06 | – |
| ash | 2.02 | 1.58 | 2.13 | – | – |
| moisture | (5.29) | 26.13 | – | – | – |
| total | 100 | 100 | 100 | 100 | 100 |
| Air classified 10 Hz | AD | AR | D | DAF | CHO |
| FC | 19.92 | 15.54 | 20.66 | 20.86 | – |
| VM | 75.59 | 58.96 | 78.39 | 79.14 | – |
| ash | 0.92 | 0.72 | 0.95 | – | – |
| moisture | 3.57 | 24.78 | – | – | – |
| total | 100 | 100 | 100 | 100 | – |
| C | 50.16 | 39.12 | 52.02 | 52.52 | 52.74 |
| H | 6.46 | 4.73 | 6.28 | 6.35 | 6.37 |
| O | 42.06 | 30.33 | 40.33 | 40.72 | 40.89 |
| N | 0.37 | 0.29 | 0.38 | 0.39 | – |
| S | 0.03 | 0.02 | 0.03 | 0.03 | – |
| ash | 0.92 | 0.72 | 0.95 | – | – |
| moisture | (3.57) | 24.78 | – | – | – |
| total | 100 | 100 | 100 | 100 | 100 |
| Air classified 28 Hz | AD | AR | D | DAF | CHO |
| FC | 18.68 | 14.57 | 19.54 | 19.67 | – |
| VM | 76.31 | 59.52 | 79.83 | 80.34 | – |
| ash | 0.61 | 0.48 | 0.64 | – | – |
| moisture | 4.41 | 25.44 | – | – | – |
| total | 100.01 | 100.01 | 100.01 | 100.01 | – |
| C | 48.93 | 38.17 | 51.19 | 51.52 | 51.67 |
| H | 6.42 | 4.62 | 6.20 | 6.24 | 6.26 |
| O | 43.77 | 31.09 | 41.69 | 41.96 | 42.08 |
| N | 0.26 | 0.20 | 0.27 | 0.27 | – |
| S | 0.02 | 0.02 | 0.02 | 0.02 | – |
| ash | 0.61 | 0.48 | 0.64 | – | – |
| moisture | (4.41) | 25.44 | – | – | – |
| total | 100.01 | 100.01 | 100.01 | 100.01 | 100.01 |
| Whole tree 13 yr | AD | AR | D | DAF | CHO |
| FC | 19.15 | 14.94 | 19.89 | 19.98 | – |
| VM | 76.72 | 59.84 | 79.68 | 80.04 | – |

| | | | | | |
|------------------------|-----------|-----------|----------|------------|------------|
| ash | 0.44 | 0.34 | 0.46 | – | – |
| moisture | 3.71 | 24.89 | – | – | – |
| total | 100.02 | 100.02 | 100.02 | 100.02 | – |
| C | 49.32 | 38.47 | 51.22 | 51.46 | 51.63 |
| H | 6.44 | 4.70 | 6.26 | 6.29 | 6.31 |
| O | 43.48 | 31.34 | 41.73 | 41.93 | 42.07 |
| N | 0.30 | 0.23 | 0.31 | 0.31 | – |
| S | 0.02 | 0.02 | 0.02 | 0.02 | – |
| ash | 0.44 | 0.34 | 0.46 | – | – |
| moisture | (3.71) | 24.89 | – | – | – |
| total | 100 | 100 | 100 | 100 | 100 |
| Stem wood 13 yr | AD | AR | D | DAF | CHO |
| FC | 18.60 | 14.51 | 19.13 | 19.19 | – |
| VM | 78.37 | 61.13 | 80.59 | 80.84 | – |
| ash | 0.30 | 0.23 | 0.31 | – | – |
| moisture | 2.75 | 24.14 | – | – | – |
| total | 100.02 | 100.02 | 100.02 | 100.02 | – |
| C | 49.40 | 38.53 | 50.80 | 50.95 | 51.07 |
| H | 6.41 | 4.76 | 6.27 | 6.29 | 6.31 |
| O | 43.68 | 32.17 | 42.40 | 42.54 | 42.63 |
| N | 0.21 | 0.16 | 0.22 | 0.22 | – |
| S | 0.01 | 0.01 | 0.01 | 0.01 | – |
| ash | 0.30 | 0.23 | 0.31 | – | – |
| moisture | (2.75) | 24.14 | – | – | – |
| total | 100.01 | 100.01 | 100.01 | 100.01 | 100.01 |

Using the chemical analysis measurement data from Tables 5 and 6, the dry ash-free basis (DAF) values are calculated using Equation 10. The DAF values are shown in Tables 13 and 14. These values represent the measured cellulose, hemicellulose, and lignin fractions used in the optimization procedure for the biomass composition.

Table 13: Chemical analysis values calculated as weight percent (wt. %) dry ash-free basis (DAF).

| Chemical component | Residues | Stem wood | Bark | Needles | Bark + needles | Residues (rep 1) |
|---------------------|----------|-----------|-------|---------|----------------|------------------|
| water extractives | 5.05 | 2.72 | 2.90 | 6.29 | 4.21 | 6.40 |
| ethanol extractives | 0.64 | 0.31 | 0.46 | 1.43 | 1.03 | 0.70 |
| acetone extractives | 6.79 | 2.54 | 3.33 | 7.77 | 5.81 | 8.16 |
| lignin | 36.53 | 30.29 | 34.29 | 43.35 | 48.2 | 36.49 |
| glucan | 28.98 | 39.31 | 33.78 | 23.59 | 23.9 | 27.44 |
| xylan | 7.54 | 6.22 | 7.73 | 4.35 | 4.38 | 6.76 |
| galactan | 3.66 | 2.56 | 3.67 | 2.72 | 3.45 | 3.56 |
| arabinan | 1.98 | 0 | 3.50 | 1.61 | 2.52 | 2.94 |
| mannan | 7.86 | 14.74 | 9.14 | 7.86 | 5.62 | 6.56 |
| acetyl | 0.98 | 1.33 | 1.21 | 1.04 | 0.85 | 0.97 |
| total | 100 | 100 | 100 | 100 | 100 | 100 |

Table 14: Chemical analysis values calculated as weight percent (wt. %) dry ash-free basis (DAF).

| Chemical component | Residues:bark:needles 1:1:1 | Residues:bark:needles 1:2:2 | Air classified (10 Hz) | Air classified (28 Hz) | Whole tree (13 yr) | Stem wood (13 yr) |
|---------------------|-----------------------------|-----------------------------|------------------------|------------------------|--------------------|-------------------|
| water extractives | 5.93 | 5.79 | 3.31 | 1.76 | 2.93 | 1.53 |
| ethanol extractives | 1.05 | 1.09 | 0.45 | 0.31 | 0.46 | 0.33 |
| acetone extractives | 7.07 | 6.81 | 4.08 | 2.40 | 3.36 | 1.73 |
| lignin | 43.28 | 44.89 | 35.60 | 35.23 | 33.63 | 32.80 |
| glucan | 24.05 | 23.98 | 32.44 | 34.37 | 34.12 | 37.46 |
| xylan | 5.22 | 4.86 | 7.74 | 8.39 | 7.81 | 7.83 |
| galactan | 3.04 | 3.17 | 3.68 | 3.90 | 3.71 | 3.56 |
| arabinan | 1.67 | 2.33 | 1.36 | 0 | 3.53 | 3.47 |
| mannan | 7.77 | 6.18 | 10.15 | 12.41 | 9.23 | 9.90 |
| acetyl | 0.93 | 0.89 | 1.20 | 1.24 | 1.22 | 1.38 |
| total | 100 | 100 | 100 | 100 | 100 | 100 |

Table 15 presents the biomass compositions for each feedstock that are suitable to use with the Debiagi et al. kinetics scheme. Chemical analysis values are listed in the Measured column while values from the biomass characterization procedure using the optimized splitting parameters are given in the Estimated column. As seen in the table, the optimization procedure is able to determine the appropriate splitting parameters when comparing the biomass composition to chemical analysis data. The biomass composition for the bark feedstock is the only composition that does not compare within 1% of the chemical analysis measurements.

Table 15: Estimated biomass composition for each feedstock on a dry ash-free basis (DAF).

| Residues, Cycle 1 | Measured | Estimated |
|-------------------|----------|-----------|
| cellulose | 28.98 | 28.98 |
| hemicellulose | 22.02 | 22.02 |
| lignin-c | – | 0.58 |
| lignin-h | – | 8.79 |
| lignin-o | – | 27.16 |
| tannins | – | 1.60 |

| | | |
|---------------|-------|-------|
| triglycerides | – | 10.88 |
| total lignin | 36.53 | 36.53 |

C = 53.31, H = 6.41

$\alpha = 0.5175$, $\beta = 0.8996$, $\gamma = 1$, $\delta = 0.6486$, $\epsilon = 0.9246$

| Stem wood, Cycle 2 | Measured | Estimated |
|--------------------|----------|-----------|
| cellulose | 39.31 | 39.91 |
| hemicellulose | 24.84 | 25.42 |
| lignin-c | – | 0.89 |
| lignin-h | – | 26.20 |
| lignin-o | – | 3.20 |
| tannins | – | 0.01 |
| triglycerides | – | 4.37 |
| total lignin | 30.29 | 30.29 |

C = 50.94, H = 6.39

$\alpha = 0.5613$, $\beta = 0.981$, $\gamma = 0.7683$, $\delta = 0.9263$, $\epsilon = 0.9958$

| Bark, Cycle 3 | Measured | Estimated |
|---------------|----------|-----------|
| cellulose | 33.78 | 31.38 |
| hemicellulose | 25.24 | 22.99 |
| lignin-c | – | 35.14 |
| lignin-h | – | 0 |
| lignin-o | – | 0 |
| tannins | – | 7.15 |
| triglycerides | – | 3.34 |
| total lignin | 34.29 | 35.14 |

C = 55.69, H = 5.89

$\alpha = 0.5265$, $\beta = 0.3359$, $\gamma = 0$, $\delta = 0$, $\epsilon = 0.8527$

| Needles, Cycle 4 | Measured | Estimated |
|------------------|----------|-----------|
| cellulose | 23.59 | 23.59 |
| hemicellulose | 17.57 | 17.57 |
| lignin-c | – | 0.63 |
| lignin-h | – | 5.43 |
| lignin-o | – | 37.30 |
| tannins | – | 3.00 |
| triglycerides | – | 12.48 |
| total lignin | 43.35 | 43.35 |

C = 54.71, H = 6.36

$$\alpha = 0.5225, \beta = 0.8364, \gamma = 1, \delta = 0.5167, \epsilon = 0.8996$$

| Bark + needles, Cycle 5 | Measured | Estimated |
|--------------------------------|----------|-----------|
| cellulose | 23.91 | 23.91 |
| hemicellulose | 16.82 | 16.82 |
| lignin-c | – | 6.94 |
| lignin-h | – | 6.74 |
| lignin-o | – | 34.53 |
| tannins | – | 2.84 |
| triglycerides | – | 8.22 |
| total lignin | 48.21 | 48.21 |

$$C = 54.79, H = 6.13$$

$$\alpha = 0.5366, \beta = 0.7312, \gamma = 0.7942, \delta = 0.6975, \epsilon = 0.9169$$

| Residues (rep 1), Cycle 8 | Measured | Estimated |
|----------------------------------|----------|-----------|
| cellulose | 27.44 | 27.45 |
| hemicellulose | 20.80 | 20.81 |
| lignin-c | – | 0 |
| lignin-h | – | 3.71 |
| lignin-o | – | 32.79 |
| tannins | – | 1.98 |
| triglycerides | – | 13.27 |
| total lignin | 36.49 | 36.50 |

$$C = 53.85, H = 6.46$$

$$\alpha = 0.5181, \beta = 1, \gamma = 1, \delta = 0.365, \epsilon = 0.9228$$

| Residues:bark:needles 1:1:1, Cycle 10 | Measured | Estimated |
|--|----------|-----------|
| cellulose | 24.05 | 24.05 |
| hemicellulose | 18.62 | 18.62 |
| lignin-c | – | 7.27 |
| lignin-h | – | 3.93 |
| lignin-o | – | 32.08 |
| tannins | – | 3.89 |
| triglycerides | – | 10.16 |
| total lignin | 43.28 | 43.28 |

$$C = 54.91, H = 6.22$$

$$\alpha = 0.5128, \beta = 0.6851, \gamma = 0.7597, \delta = 0.5375, \epsilon = 0.8866$$

| Residues:bark:needles 1:2:2, Cycle 11 | Measured | Estimated |
|--|----------|-----------|
| cellulose | 23.98 | 23.99 |

| | | |
|---------------|-------|-------|
| hemicellulose | 17.43 | 17.43 |
| lignin-c | – | 10.51 |
| lignin-h | – | 3.27 |
| lignin-o | – | 31.12 |
| tannins | – | 4.59 |
| triglycerides | – | 9.10 |
| total lignin | 44.89 | 44.89 |

C = 55.25, H = 6.14

$\alpha = 0.5285$, $\beta = 0.6664$, $\gamma = 0.6661$, $\delta = 0.5255$, $\epsilon = 0.88$

| Air classified (10 Hz), Cycle 12 | Measured | Estimated |
|---|----------|-----------|
| cellulose | 32.44 | 32.44 |
| hemicellulose | 24.13 | 24.13 |
| lignin-c | – | 4.82 |
| lignin-h | – | 13.86 |
| lignin-o | – | 16.93 |
| tannins | – | 0 |
| triglycerides | – | 7.83 |
| total lignin | 35.60 | 35.60 |

C = 52.74, H = 6.37

$\alpha = 0.5228$, $\beta = 0.7661$, $\gamma = 0.8174$, $\delta = 0.8261$, $\epsilon = 1$

| Air classified (28 Hz), Cycle 13 | Measured | Estimated |
|---|----------|-----------|
| cellulose | 34.37 | 34.37 |
| hemicellulose | 25.94 | 25.94 |
| lignin-c | – | 3.76 |
| lignin-h | – | 18.38 |
| lignin-o | – | 13.09 |
| tannins | – | 0 |
| triglycerides | – | 4.46 |
| total lignin | 35.23 | 35.23 |

C = 51.67, H = 6.26

$\alpha = 0.5191$, $\beta = 0.8365$, $\gamma = 0.8302$, $\delta = 0.9101$, $\epsilon = 0.9996$

| Whole tree (13 yr), Cycle 15 | Measured | Estimated |
|-------------------------------------|----------|-----------|
| cellulose | 34.12 | 34.13 |
| hemicellulose | 25.50 | 25.50 |
| lignin-c | – | 0.91 |
| lignin-h | – | 16.12 |
| lignin-o | – | 16.60 |

| | | |
|---------------|-------|-------|
| tannins | – | 0.66 |
| triglycerides | – | 6.08 |
| total lignin | 33.63 | 33.63 |

C = 51.63, H = 6.31

$\alpha = 0.5216$, $\beta = 1$, $\gamma = 0.9175$, $\delta = 0.845$, $\epsilon = 0.9517$

| Stem wood (13 yr), Cycle 16 | Measured | Estimated |
|------------------------------------|----------|-----------|
| cellulose | 37.46 | 37.46 |
| hemicellulose | 26.14 | 26.14 |
| lignin-c | – | 1.84 |
| lignin-h | – | 24.58 |
| lignin-o | – | 6.38 |
| tannins | – | 0.01 |
| triglycerides | – | 3.59 |
| total lignin | 32.80 | 32.80 |

C = 51.07, H = 6.31

$\alpha = 0.5387$, $\beta = 0.9443$, $\gamma = 0.7995$, $\delta = 0.9372$, $\epsilon = 0.9991$

The biomass characterization of the Residues feedstock is visually shown in Figure 12. The feedstock's carbon-to-hydrogen ratio (CHO basis) obtained from chemical analysis data is marked with a triangle symbol. The reference mixtures obtained from the optimized splitting parameters are marked with square symbols that bound the feedstock with a dashed line.

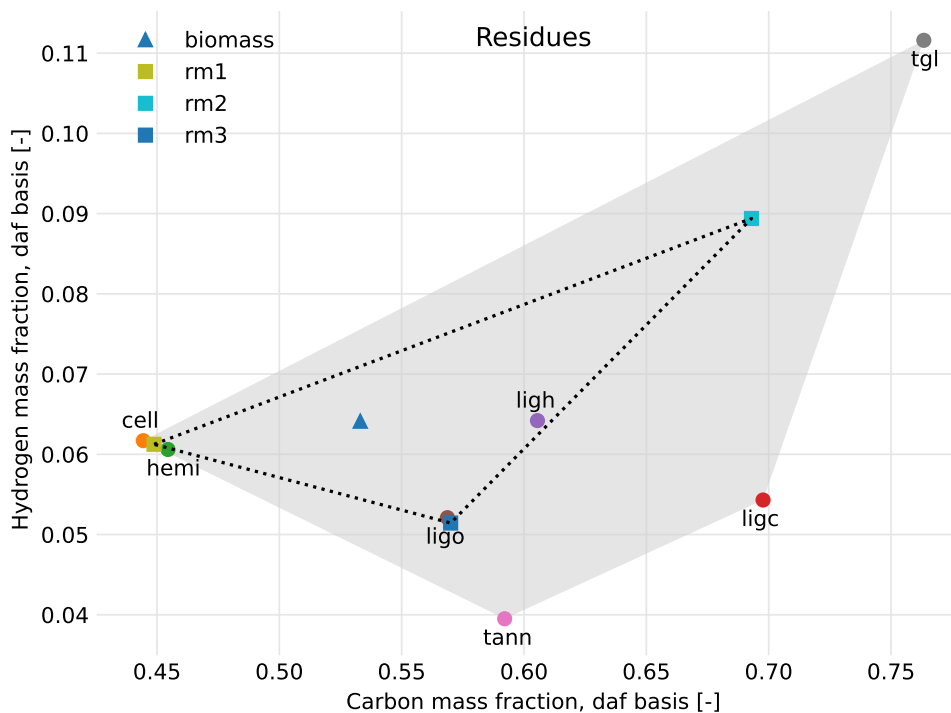


Figure 12: Characterization of the Residues feedstock using ultimate analysis data, chemical analysis data, and optimized splitting parameters.

4.2 Batch reactor model

To understand the time-scale and conversion profiles associated with the Debiagi biomass pyrolysis kinetics, the batch reactor model was implemented with the Residues feedstock. Reaction time in the batch model was set to 20 s, a constant reaction temperature of 773.15 K, and a pressure of 101,325 Pa. Figure 13 displays the conversion of the initial biomass concentration with respect to time. All biomass fractions are converted to products within 10 s except for the tannins. All pyrolysis products appear to be generated within 10 s of reaction time as demonstrated by Figure 14. Final mixture yields are approximately 15 wt. % gas, 57 wt. % liquids, 13 wt. % solids, and 14 wt. % metaplastics which suggests a total solids yield of 27 wt. %.

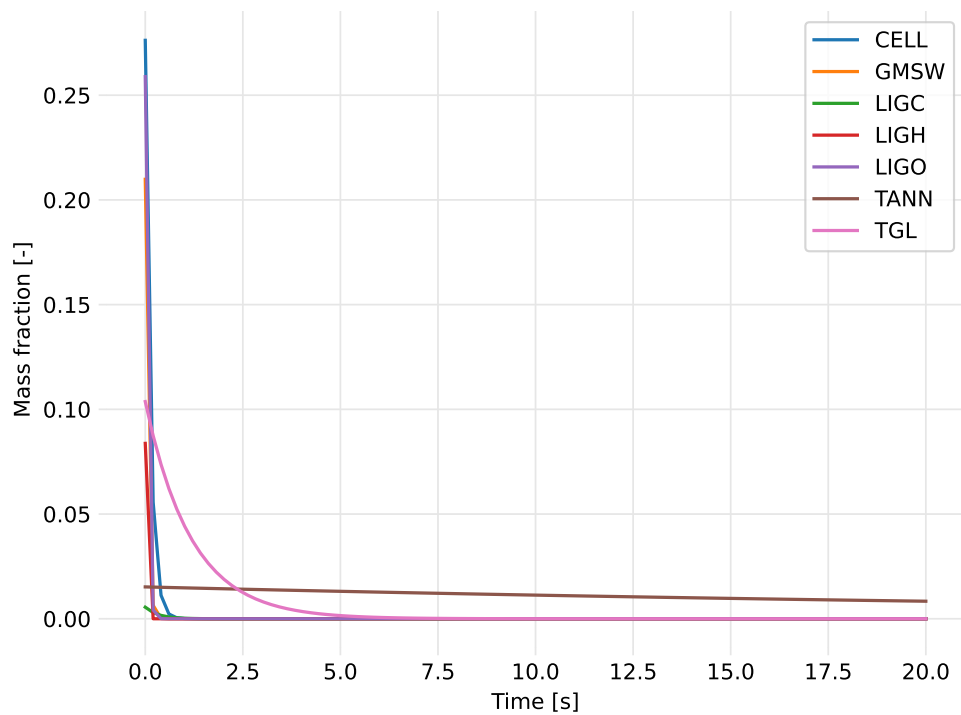


Figure 13: Conversion profiles of the biomass composition for the Residues feedstock.

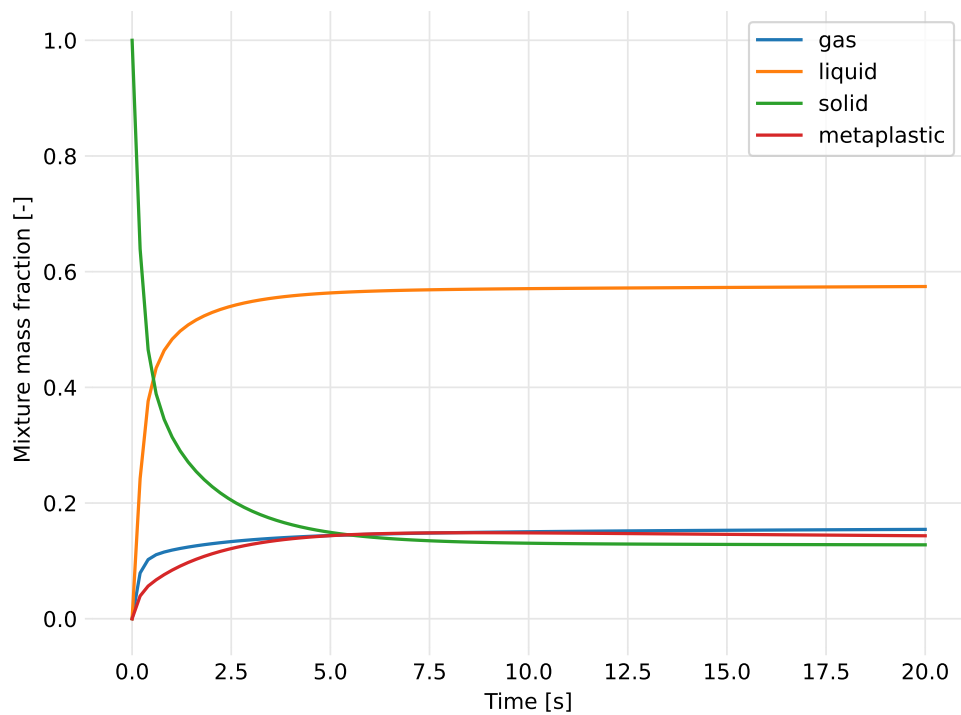


Figure 14: Generation of the pyrolysis products for the Residues feedstock.

According to the experimental data from the NREL 2FBR, the char yield for the Residues feedstock is around 15 wt. % compared to the batch reactor model's 27 wt. % total solids yield. A majority of the solids yield from the batch reactor model is due to the metaplastic species. To increase the metaplastic reaction rates, temperature T was added to the prefactors. For example, the original prefactor for reaction 23 in Table 9 is 5×10^{12} while the modified prefactor is $5 \times T \times 10^{12}$. The effects of this modification can be seen in Figure 15 where the metaplastic yield for the Residues feedstock is considerably less than the yield from the original reaction rates. Total solids yield using the modified reaction rates is approximately 18 wt. % compared to 27 wt. % using the original reaction rates. The remaining reactor models presented in this report use the modified metaplastic reaction rates since the total solids yield more closely resembles the NREL 2FBR char yield.

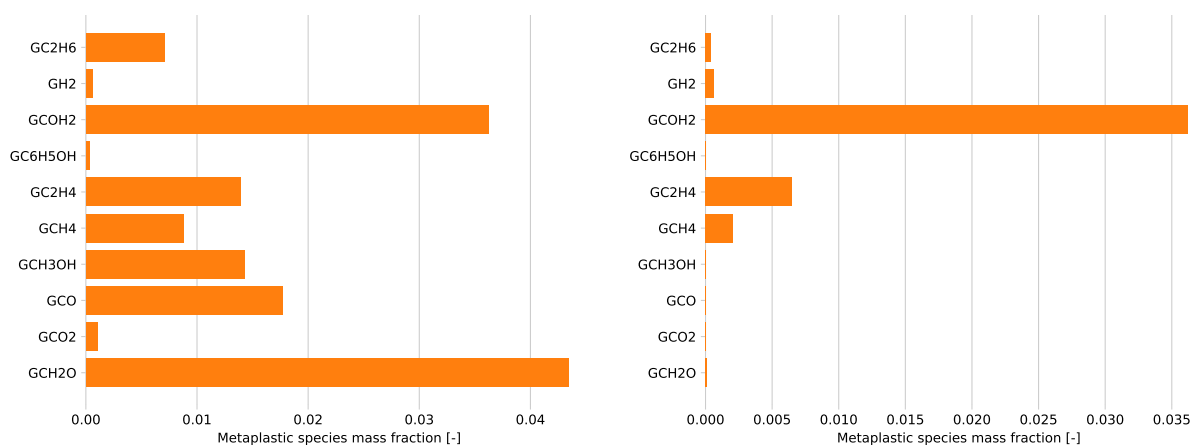


Figure 15: Metaplastic yields for the Residues feedstock using the original (left) and modified (right) reaction rates in a batch reactor model.

To compare the experimental yields to the reactor model results, the measured products from the NREL 2FBR are lumped into gases, liquids, and solids. Gases represent the light gas, condensables, and water vapor products. Liquids are the oil yield and solids are the char yield. Solids from the model are represented by the solid and metaplastic species. Figure 16 compares the yields from the NREL 2FBR fluidized bed reactor to the batch reactor model. The batch reactor model results are within 10% of the experimental yields.

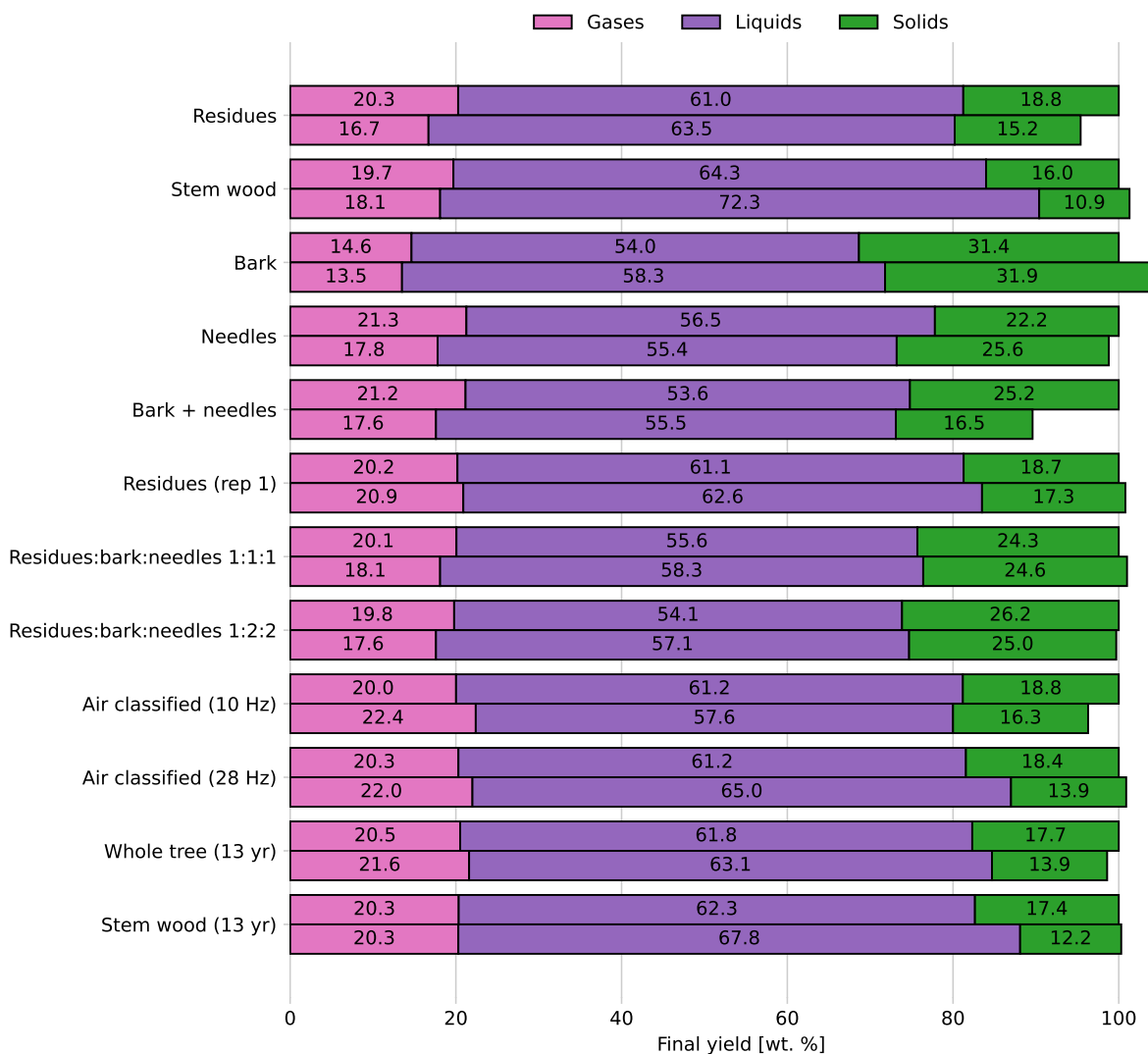


Figure 16: Comparison of the experimental yields and the batch reactor model results. For each feedstock, model results are the top bar and experimental yields are the bottom bar.

A comparison of the lumped yields to ash content in the feedstocks is shown in Figure 17. The experimental data and batch reactor model suggest a decrease in liquids (oil) yield with increasing ash content. The data and model also suggest a higher solids yield for increased ash content. Trends for the experimental data and model do not agree for the gases. Overall, the batch reactor model is able to qualitatively capture the effects of ash content on pyrolysis yields due to ash content in the biomass feedstock.

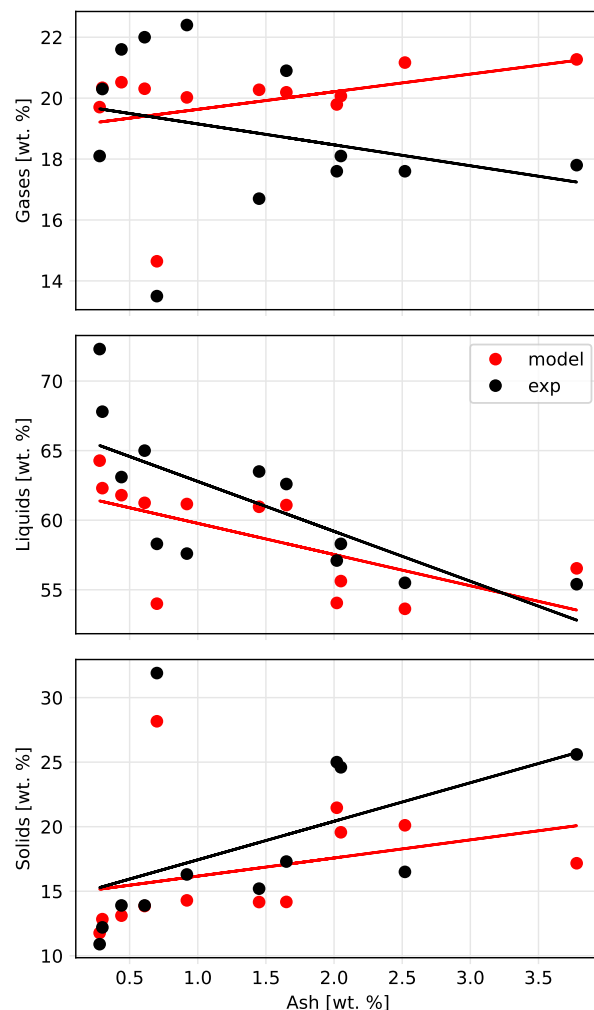


Figure 17: Comparison of the experimental and batch reactor model yields to feedstock ash content.

The Debiagi et al. kinetics scheme makes it possible to predict individual components of the pyrolysis products. Yields for several chemical species generated from each feedstock using the batch reactor model are given in Figure 18. The stem wood produced the largest mass fraction of acetaldehyde, acetic acid, and furfural. The bark plus needles feedstock generated the highest yield of formaldehyde. Needles produced the highest mass fraction for the heavy molecular weight lignin. Bark generated the largest yield of phenol and did not produce any noticeable amount of the heavy lignin.

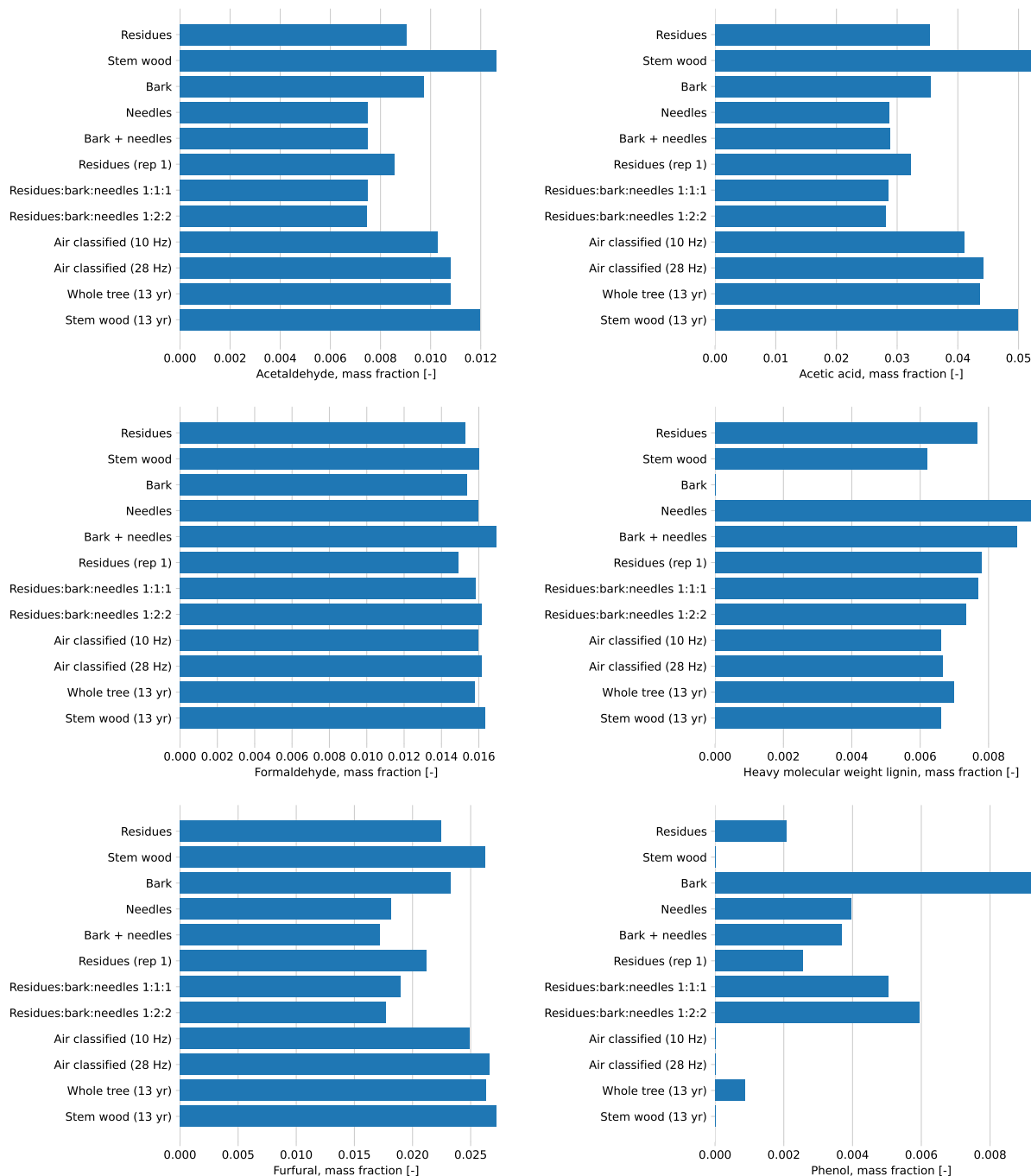


Figure 18: Chemical species yields from the batch reactor model.

The effects of reactor temperature on product yields are shown in Figure 19. Increasing the reaction temperature above 773.15 K (500°C) improves the rate of conversion; consequently, a higher reactor temperature should be used if the feedstock residence time is less than 5 to 10 seconds. At temperatures less than 773.15 K, a feedstock residence time greater than 10 seconds may be needed for full devolatilization of the biomass. It should be noted that the Debiagi et al. kinetics does not account for secondary reactions

of the pyrolysis products. Therefore, the batch reactor model does not currently capture the effects of long residence times.

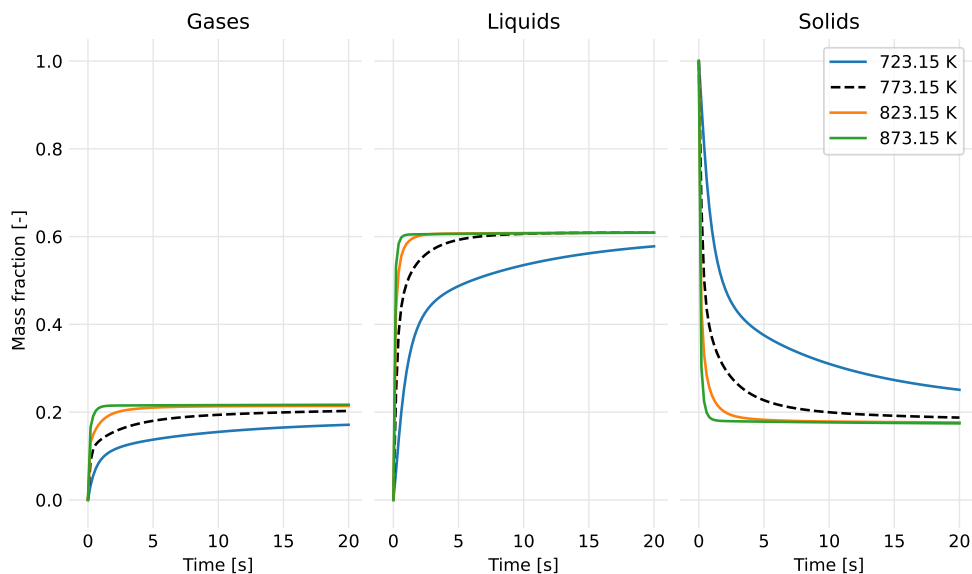


Figure 19: Batch reactor model yields at different reaction temperatures. Dashed line represents the NREL 2FBR temperature.

4.3 CSTR model

Here.

5 Conclusions

Here.

6 Hardware requirements

The reduced order models discussed in this report were developed and executed on a MacBook Pro laptop (see hardware specs below). The models do not give as much detail as full 3D simulations but they provide good enough results in a timely manner; as such, they lend themselves well to process modeling, design of experiments, and rapid prototyping tasks.

- MacBook Pro, 16-inch, 2019 model
- 2.3 GHz 8-core Intel i9 CPU
- 32 GB 2667 MHz DDR4 memory

- 4 GB AMD Radeon Pro 5500M GPU
- macOS Big Sur version 11.6

7 Source code and web application

Source code for this project is available on GitHub at the link provided below. See the README markdown document in the repository for more information.

- <https://github.com/wigging/fcic-pyrolysis>

A web application was developed based on the biomass compositional work discussed in this report. The application is an online tool for calculating biomass composition from ultimate and chemical analysis data. The resulting composition can be used with reactor models that utilize the Debiagi et al. kinetics scheme [2]. The application is available at the URL given below. A screenshot of the application in a browser window is shown in Figure 20.

- <https://share.streamlit.io/wigging/biocomp/main/app.py>

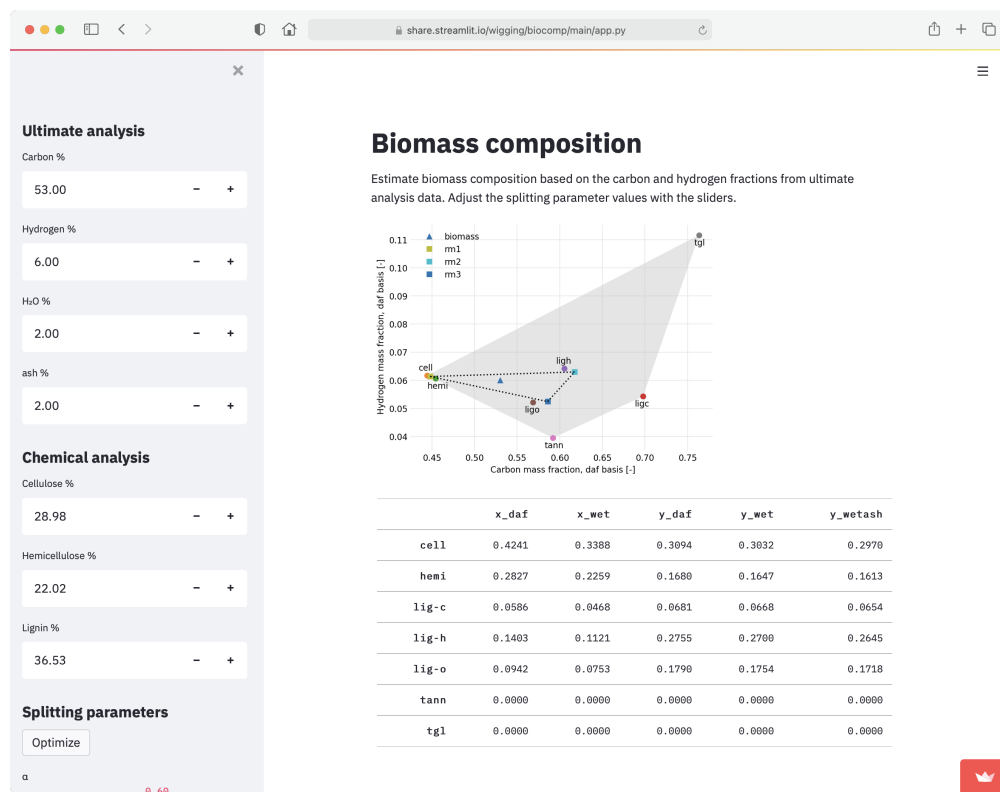


Figure 20: An online tool to estimate biomass composition from ultimate and chemical analysis data.

References

- [1] ASTM D3180-15. *Standard Practice for Calculating Coal and Coke Analyses from As-Determined to Different Bases*. West Conshohocken, PA: ASTM International, 2015.
- [2] P. Debiagi et al. “A predictive model of biochar formation and characterization”. In: *Journal of Analytical and Applied Pyrolysis* 134 (2018), pp. 326–335.
- [3] Paulo Eduardo Amaral Debiagi et al. “Extractives Extend the Applicability of Multi-step Kinetic Scheme of Biomass Pyrolysis”. In: *Energy & Fuels* 29.10 (2015), pp. 6544–6555.
- [4] Richard French and Kristiina Iisa. *Personal discussions and email correspondence*. NREL, Apr. 2019.
- [5] David G. Goodwin et al. *Cantera: An Object-oriented Software Toolkit for Chemical Kinetics, Thermodynamics, and Transport Processes*. Version 2.4.0. Aug. 2018. doi: 10.5281/zenodo.1174508. URL: <https://doi.org/10.5281/zenodo.1174508>.
- [6] William A. Rogers. Email correspondence. National Energy Technology Laboratory, May 2021.